NTNU – Trondheim
Norwegian University of
Science and Technology

Numerical Simulation of Gas Coning of a Single Well Radial in a Naturally Fractured Reservoir

Isemin Akpabio Isemin

Petroleum Engineering
Submission date: August 2012
Supervisor: Jon Kleppe, IPT

Norwegian University of Science and Technology
Department of Petroleum Engineering and Applied Geophysics

NTNU

Norwegian University of
Science and Technology

Master's Thesis:

Numerical Simulation of Gas Coning of a Single Well Radial in a Naturally Fractured Reservoir

by

Isemin Akpabio Isemin

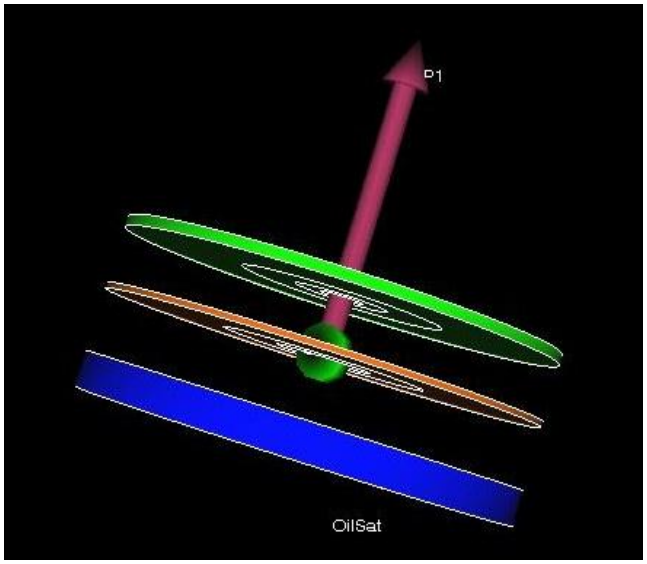

Master of Science in Reservoir Engineering

Supervisor: Professor Jon Kleppe

Co-Supervisor: Dr Hassan Karimaie

Spring, 2012

Norwegian University of Science and Technology

Department of Petroleum Engineering and Applied Geophysics

PREFACE

This THESIS is carried out in spring, 2012 of the final semester of the Master of Science programme under the supervision of Professor Jon Kleppe and co-supervised by Dr Hassan Karimaie both of the Department of Petroleum and Applied Geophysics, Norwegian University of Science and Technology (NTNU).

Special thanks to Professor Pål Skalle and Dr Uduak Mme for their contribution.

June, 2012

Isemin A. Isemin
isemin@stud.ntnu.no

DEDICATION

This THESIS work is dedicated to the family of Mr and Mrs Akpabio J. Isemin and to the organisers of the EnPe - NORAD's programme for the finance, support and prayers.

God Bless You All

ACKNOWLEDGEMENT

My sincere appreciation goes to my supervisor Professor Jon Kleppe (Head of the Department for Petroleum Engineering and Applied Geophysics at NTNU) and Co-supervisor Dr Hassan Karimaie for their valuable and constructive suggestions during the planning and development of this THESIS work that has become a reality.

I'm particularly grateful for the assistance and opportunity accorded me from start-to-finish of this MSc through the EnPe - NORAD'S Programme for Energy and Petroleum, NTNU, Norway.

Special thanks also to the authors mentioned in the reference whose materials I found in articles or in books for use.

I sincerely thank my parents Mr and Mrs Akpabio J. Isemin, my siblings (Grace, Ime, James and JayDee) and those whom names are not mentioned: for their prayers and support.

Above all, I could not have completed this thesis without the help of God Almighty whose love and mercies is sufficient and gracious during the period of this great MSc programme.

ABSTRACT

Gas coning is the tendency of the gas to drive oil downward in an inverse cone due to the downward movement of gas into the perforations of a producing well thereby reducing oil production and the overall recovery efficiency of the oil reservoir. This work addresses gas coning issues in a naturally fractured reservoir via a numerical simulation approach on a single-well radial cross-section using the ECLIPSE 100 reservoir simulator. Matrix and fracture properties are modelled. Critical rate, breakthrough time and GOR after breakthrough is determined which is used to investigate the effect of matrix and fracture properties on gas coning effective reservoir parameters such as oil flow rate, matrix and fracture porosity, vertical and horizontal matrix and fracture permeability, matrix block size, etc. Results show that reservoir parameters that affect coning include oil flow rate, matrix and fracture porosity, matrix and vertical permeability, anisotropy ratio, perforated interval thickness, density difference and mobility ratio. While matrix block size and fracture spacing have no significant effect on gas coning.

TABLE OF CONTENT

LIST OF FIGURES

LIST OF TABLES

1.0 INTRODUCTION

Gas coning pose a big problem in many oil field applications as it significantly reduces oil production, increase cost of production operation and has a direct effect on the overall recovery efficiency of the oil reservoirs. This is as a result of an imbalance between the gravitational and viscous forces around the completion interval of an oil reservoir where a large oil rate causes a downward coning of gas into the perforations of a producing well whenever there is a change in Gas-Oil Contact (GOC) profile. These said oil reservoirs are prone to gas coning and the oil will be produced by the use of long horizontal perforated well. When the gas gets to the production well, it starts dominating the flow in the well thus decreasing the oil production. Factors like critical production rate, breakthrough time, and well performance after breakthrough could aid the coning problem.

Gas coning in naturally fractured reservoirs is presented herein this work. The concept of gas cone development in naturally fractured reservoirs (NFR) is traceable to fracture patterns around a producing well. The development follows the path of least resistance flow unless an assumption of uniformity is considered with respect to fracture permeability and fracture orientation. Cone breakthrough occurs through the fracture into the well when production rate is increased which results in more gas being produced.

Factors like vertical and horizontal permeability plays a vital role in gas coning in NFR. A high vertical permeability in fractures is bound to accelerate the coning process resulting in lowering the critical rate and more rapid breakthrough time. Irrespective of structural position, wells are still affected as the fluid prefers to flow through fracture and the uneven fracture conductivities commonly observed in NFR is depleted.

A radial system is used in this coning study since small blocks adjacent the wellbore provide accurate modelling of cone shape. Coning development in NFR is described below.

1.1 CONING DEVELOPMENT

Shown in Fig. 1 is original reservoir at static condition. When oil is being produced from the reservoir (assuming the well is partially penetrating the formation so that the production interval is halfway between the fluid contact), it results to pressure drawdown thus lowering the gas-oil contact (and elevate the water-oil contact) in the well environs. Oil production reduces in the process due to gas mobility that is much higher than the oil mobility thereby making gas flow to be more dominant than the oil flow. The pressure drawdown near the wellbore causes the gas which is the more mobile phase to move faster than the oil which is

the less mobile phase into the perforation interval. If the pressure drawdown exceeds the hydrostatic pressure differential between oil and gas, the fluid will also be drawn towards the well resulting for the gas-oil interface to rise in a shape of a CONE for a homogeneous oil zone overlain by gas as show in Fig. 2**.** Meyer and Garder (1954) suggest that coning development is a result of the radial flow of the oil and an associated pressure sink around the wellbore.

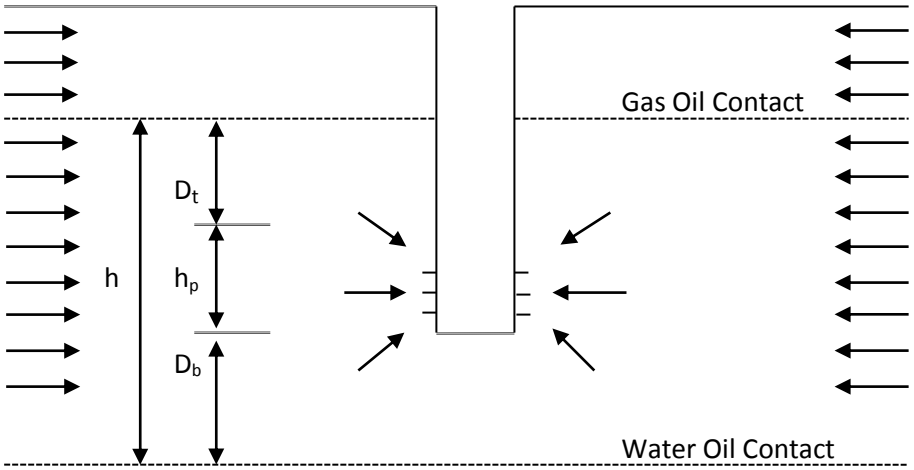

Figure 1.1: Original reservoir static condition

Fig. 3 represents a model where a reservoir which is equipped with a horizontal production well located in the middle of thin oil rims tends to experience coning. Oil can be produced by the use of long horizontal perforated well for reservoirs that are prone to gas coning as represented in Fig. 3. When viscous forces at the wellbore exceed gravitational forces, a cone will ultimately break into the well. Gravity for is one of the essential forces that may affect the fluid flow distribution around the wellbore, a brief description of gravity mechanism in naturally fractured reservoir is presented in section 1.7.

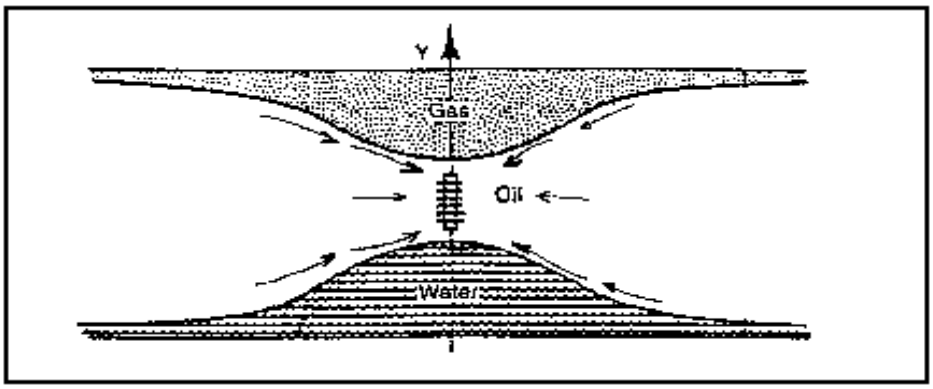

Figure 1.2: Gas and Water Coning

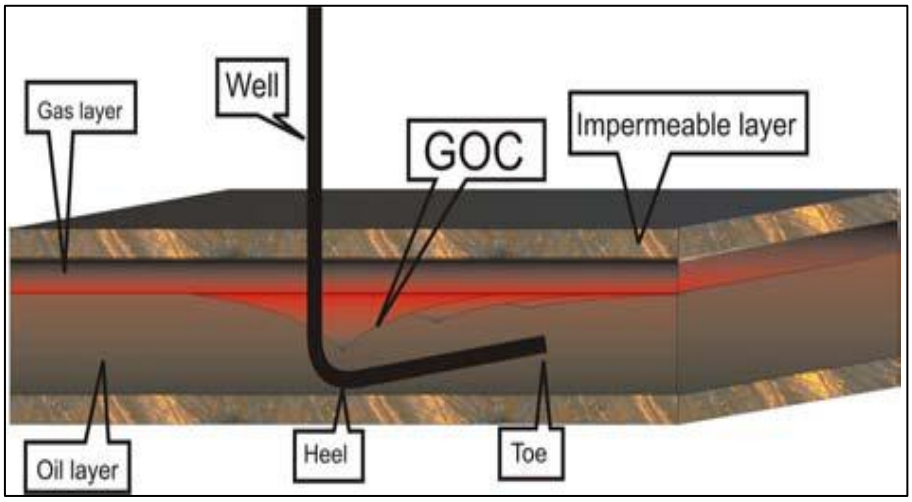

Figure 1.3: GOC profile in a reservoir with a horizontal well

1.2 PINCIPLES OF CONING PHENOMENA

Since coning reduces well productivity, there exist some practices that are adopted to delay coning with the main aim of maximizing reserves which include:

1.2.1 WELL SPACING

There is a finite cone area at the base of the cone that is effectively drained in gas-oil system, so placing adjacent wells in the pool so that their cones do not interfere with each other helps to drain the pool more effectively.

1.2.2 COMPLETION INTERVALS

Maximizing stand-off from fluid contacts since reserves drained by vertical wells vary with the cube of the stand-off. Consideration is that completions have to be in a highly porous and permeable interval shielded by a tight layer that will help reduce coning. In a case of an oil sandwich producing under a double coning situation, an appropriate interval such that both cones breakthrough at about the same time may be selected so as to reduce coning.

1.2.3 PRODUCTION PRACTICES

Production must occur below critical rates if a large amount of gas is unacceptable for environmental, regulatory, or equipment constraint reasons. If above mentioned factors are not critical and does not affect production, then production must occur at a rate that will optimize cash flow and reserves.

1.3 CONING PROBLEM

Coning models are subject to instability because of their convergent nature of the flow pattern. The pore volume of the individual grid blocks typically decrease sharply near the wellbore in part due to the cylindrical geometry and in part due to the use of small radial grid spacing near the wellbore. During and after breakthrough of the displacing space, the relative amount of each phase flowing into and out of a block are determined by the saturations in that block and in the adjacent gridblock. These saturations are known only for the beginning of the time interval. If the relative flow of one phase into a block increases sharply, the use of the out-of-date saturation to compute the relative flow out of the block will result in the calculation of unrealistic high values for the updated saturation. When the computations are continued to the next time step, just the opposite happens and a low saturation is found. The oscillation in saturation will continue in subsequent calculations yielding meaningless results. Other gas coning problems include: costly gas handling, gas production from the original or secondary gas reduces pressure without obtaining the displacement effects associated with gas drive, reduced efficiency of the depletion mechanism and/or loss of the total field overall recovery.

1.3.1 EFFECT OF RESERVOIR HETEROGEINETY (FRACTURE) ON GAS CONING

Reservoir heterogeneity on gas coning causes a rapid cone breakthrough which results in reducing the production rate thus making oil production uneconomical. Due to the presence of fractures, near-wellbore modelling of two phase flow in different directions for matrix and fracture is a better option for coning studies in NFR using a radial system since small blocks adjacent the wellbore will provide accurate modelling of cone shape as used in these studies. Non-uniform fracture distribution and heterogeneity in NFRs make cone development asymmetrical and estimation of critical rate and breakthrough time requires modelling with an understanding of fracture pattern around the producing well otherwise, the fracture patterns together with high values of vertical permeabilities in fractures will yield a rapid non-uniform paths for cone development of least resistance flow unless an assumption of uniformity is considered with respect to fracture permeability and fracture orientation.

1.3.2 EFFECTIVE PARAMETERS ON GAS CONING

The main parameters considered has having effect on gas coning include among others: oil flow rate, matrix and fracture porosities, horizontal and vertical permeabilities in matrix and fractures, fracture spacing, mobility ratio, oil reservoir thickness, matrix block size in vertical and horizontal directions, anisotropy ratio, oil and gas densities, oil and gas viscosities, etc.

1.4 METHODS OF MITIGATING CONING

Several ideas have being investigated (though not all that is implemented) either by laboratory analysis or by simulation studies but very few have being reportedly published in a field testing. However, some aforementioned listed looks promising:

1.4.1 INTRODUCTION OF EXTRANEOUS MATERIALS INTO THE RESERVOIR:

Restricting the flow of gas towards the well by introducing extraneous materials into the reservoir is a method that is achievable by injecting cementing agents, gels, polymers, or foams and is even more effective when horizontal fractures are created in the stand-off region. Another method in this category is reducing drastically the absolute permeability in the stand-off region by injecting tar or precipitating asphaltenes. Injecting oil into the gas zone places an oil barrier to gas coning is another method (Fig. 4). Lastly, introducing chemicals like foams, surfactants, and gels reduces the relative permeability to gas which helps in restricting the flow of gas towards the well.

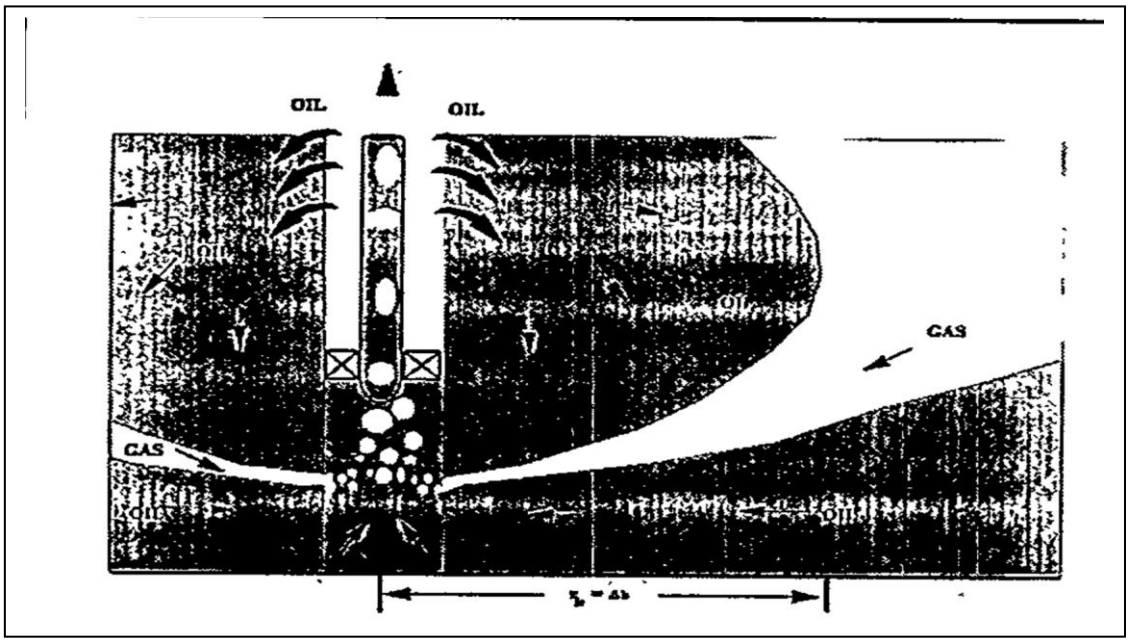

Figure 1.4: Liquid barrier to gas flow (after Richardson et. al.)

1.4.2 MODIFYING DYNAMIC PRESSURE DISTRIBUTION AROUND THE WELL

Reverse coning is one of the methods herein where oil is being produced through the water zone to mitigate gas coning. The gas then travels through zones with higher oil and water saturations, thus encountering more resistance (Fig. 5). Another method is to introduce

additional perforation in the gas zone so as to modify pressure distribution around the wellbore and relieving coning in the oil zone.

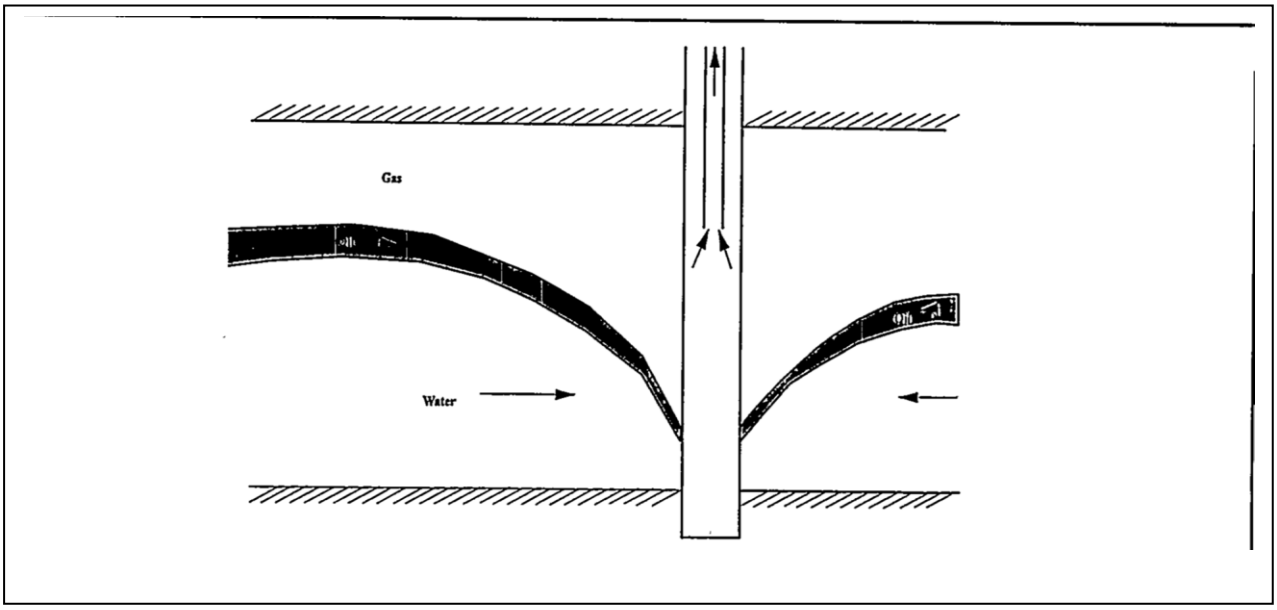

Figure 1.5: Reverse Coning (after Van Lookeren)

1.4.3 DEPLETION OF GAS ZONES

If gas zones are limited in size, then drainage of isolated waters of limited size in gas pools or in heavy oil pools may be a good option.

1.5 GRAVITY DRAINAGE MECHANISM

The fractured porous media consist of two different systems: matrix and fracture. While the matrix has high porosity and low permeability, the fracture has low porosity and high permeability that leads to early gas and water breakthrough and subsequent low displacement performance.

As production begins, reservoir pressure tends to drop thereby directly affecting the gas-oil contact in the fracture to go down below that in the matrix, and some of the oil matrix blocks become surrounded by gas. Also, when the gravitational forces exceed the capillary forces then those matrix blocks in the Gas Invaded Zone (GIZ) will undergo a gravity process. The entire process of this gravity drainage is dependent on the density difference between the oil in the matrix and the gas in the fracture thereby providing the pressure difference required for the oil recovery from the matrix block as gas enters into the block from the top while the oil is produced at the bottom. During the production of oil from the matrix block,

capillary pressure opposes the fluid exchange between the matrix block and the fracture thereby making the oil expulsion only to be possible if the height difference between the gas-oil contacts in the matrix and the fracture is greater than the capillary threshold height. If the height of the matrix block is less than the capillary threshold height then oil will not be recovered from the matrix block unless there is a capillary continuity between them.

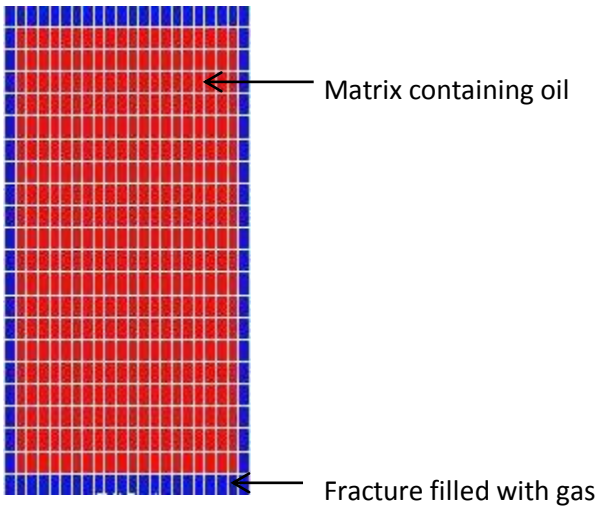

Figure 1.6: schematics of fracture-matrix model using Eclipse 100

As shown in figure 6 above is a schematic of a single matrix block that is surrounded by gas in fractures. Gravity force tends to drain the oil from the matrix block and capillary forces tend to retain the oil.

1.6 RESERVOIR SIMULATION

Reservoir simulation is a useful tool that is widely used in field development and for reservoir description and analysis. It allows engineers and scientist to simulate their recovery schemes before implementing them on the real field. It is multi-disciplinary and incorporates effort from geosciences, geophysics, reservoir-, production- and facilities engineering, computer science and economics.

1.6.1 DEVELOPMENT OF THE GEOLOGICAL MODEL

The geological model is a static numerical representation of the reservoir, and often referred to as a geocellular model. It provides seismic structural interpretations and well petrophysical data in a numerically consistent way along with known depositional characteristics. Petrophysical properties such as porosity, permeability, and water

saturations are distributed throughout the interwell 3D volume using various techniques, many of which rely on geostatistics.

Geological models may consist of 25 to 50 million cells on large and/or geologically complex reservoirs. The ability to build detailed static geological models has outstripped the reservoir engineer's ability to simulate an equal number of cells. Geostatistics have generally been focused on defining- and describing the reservoir geology using 2D maps which depict the most likely interpretation of the depositional environment and the variability of the reservoir parameters between the wells. These interpretations have historically been referred to as "deterministic" reservoir descriptions. With the advent of geocellular models and the application of such technologies as geostatistics, it is now possible for geostatistics to generate multiple reservoir descriptions for the reservoir engineer to simulate. One of these descriptions may be selected to represent the "deterministic model". Regardless if one or several static models are handed over for reservoir simulation, it is generally necessary to reduce the cell count to run the problem with existing reservoir simulators.

Significant effort has being put to improve techniques to reduce the number of reservoir cell in the areal and vertical dimension while maintaining the essential geologic character that impacts the recovery process under consideration. This approach is referred to as upscaling.

1.6.2 UPSCALING GEOLOGICAL MODEL TO RESERVOIR FLOW MODEL

Geological models, which contain the complex structural features of large oil- and gas reservoirs, commonly have tens of millions of cells. These models, which contain pinchouts, faults, and other significant information including lithology and facies distributions, are upscaled in both the vertical and areal directions to tens of hundreds of thousands of cells for reservoir simulation. Several upscaling techniques have been developed over the years including analytical techniques, local flow-based methods, and global flow-based methods. The analytical methods uses an arithmetic, harmonic, power law, and geometric averaging to calculate effective properties foe each reservoir model gridblock. The local flow-based methods calculate effective gridblock properties by performing single-phase flow simulations in each direction across the upscaled block. Lastly, the global flow-based methods use pressure gradients across the entire field subject to a specific set of wells to calculate the permeability tensor. Both the local- and global flow-based techniques can be used to compute upscaled transmissibility's directly.

1.7 RELATED STUDIES

Studies of gas coning in naturally fractured reservoirs receives less consideration compared to conventional oil and gas reservoirs. Al-Afaleg *et al*. studied coning phenomena in naturally fractured reservoir. In their work, they proposed a correlation to account for fracture acceleration effects in computation of critical rates and the breakthrough times for uniformly distributed fractures. Their work showed that empirical correlation for homogeneous single porosity reservoirs are inapplicable to naturally fractured reservoirs and results are optimistic in estimating the breakthrough time and critical rates. Chen Huan-zhang carried out a numerical simulation of coning behaviour of a single well in a naturally fractured reservoir. A fluid-flow equation that accounts for matrix and fracture was modelled. The model developed can be used to study production from a single well. Some early work carried out in calculating the critical rate for water/gas coning for naturally fractured reservoirs were presented by J. Birks. Van Gulf-Racht and Sonier studied water-coning in a naturally fractured reservoir. Their objective was to extend the investigation to the coning criteria in a "fractured reservoir" by including the production of oil and water and not only preventing the production of water. Among the problem they examined was the role of well completion, role of reverse coning, reservoir "internal architecture" role associated with the matrix "block size", and also the role of horizontal and fracture density which is equivalent to a certain degree of anisotropy.

Gas coning process in a gas oil reservoir completed with a horizontal well was analytically modelled, simulated, and analysed by Sagatum *et al.* using a nonlinear approach under gas coning conditions. They developed a model that described the interaction between the well and the reservoir may be cast into a boundary control problem of the porous media equation with two boundary conditions. Their simulation results show significant improvement of production profit of the proposed method compared to a conventional method which usually uses a constant rate up until gas breakthrough. Renard *et al.* studied potential of multilateral wells in gas coning situations in order to confirm the merits of multilateral wells to produce oil pay in the presence of a gas cap. Their result of the numerical study corroborate that the reduction of gas coning is therefore important with the multilateral well as oil recovery was accelerated and final production greatly increased. The concept of critical rate in gas coning was done by Konieczek. He describes a critical production rate, which if exceeded, results in gas breakthrough – the cones breaks and gas is produced in addition to oil. A simplified model for the critical rate for gas coning problems in thin oil layer reservoirs was constructed in His work. He used a gravity drainage model, in which the oil flow towards the well is driven by the hydrostatic pressure gradient in the oil. Results however show that critical rates decline as a function of the cumulative production. Ekrann showed that the critical rate for coning toward a horizontal or vertical well

approaches zero at the distance to the outer open boundary approaches infinity. Ahcene and Djebbar used a numerical approach to study gas coning in vertical and horizontal wells using a 3-D irregular Cartesian model, and gas dipping using a 3-D irregular Cartesian model. At the end of their studies, they concluded that horizontal wells perform better than vertical wells in coning facing wells. A numerical simulation approach will be used in this work to study gas coning and a brief description of reservoir simulation is detailed in the next section.

Generally, gas coning model was first proposed by Muskat in 1937. The coning model equation was derived from the thermodynamics relation under isothermal expansion. Konieczek used different approach to arrive at same equation by introducing boundary conditions at the outer boundary of the well and at the well heel. A simplified model for the critical rate for gas coning problems in thin oil reservoirs was constructed by Konieczek and He used a gravity drainage model in which the oil flow towards the well is driven by the hydrostatic pressure gradient in the oil. However, there exists a well-defined GOC interface with no transition zone in His work. Mjaavatten et al., based on Konieczek work, developed a mathematical model that could predict gas coning behaviour. Though simple is a simple model structure and short computational time, the accuracy of the predictions has been good. Sagatun introduced the use of control theory in the gas coning problem using a proxy model by formulating an optimal oil production problem as a boundary control problem.

In the early documentation of critical rate studies performed by Muskat and Wyckoff assumed linear flow which has led to many researchers considering flow parameters such as permeability heterogeneity, oil zone thickness, mobility ratios etc. whereas Meyer and Garder brought forward the radial flow. J. Birks presented a calculation of critical water/gas coning for naturally fractured reservoirs.

However, the contribution of this work is to investigate gas coning in naturally fractured reservoirs so as to study coning parameters.

1.8 THESIS OBJECTIVE

The objective of this thesis is centred on a single well radial cross-section (having only one central producing well) that involves gas coning. This will be evaluated by:

i. Modelling fracture and matrix properties into a single well radial system
ii. Examining well performance through completion locations and grid block perforations of gas-oil coning

iii. Perform a sensitivity analysis of well reservoir parameters that affects gas coning using a single well radial model in ECLIPSE simulator. Parameters will include: Oil flow rate, Porosity effect, matrix and fracture permeability, Matrix block size effect, Fracture spacing, Anisotropy ratio, Perforated Interval thickness, density difference effect and Mobility ratio.

2.0 THEORETICAL ANALYSIS OF GAS CONING

2.1 GAS CONING ISSUES

Though few studies have considered gas coning in naturally fractured reservoirs there exist a lot of mathematical correlations in the conventional oil and gas reservoirs. Critical rate, breakthrough time and well performance after breakthrough are key issues in the gas coning process in both the conventional reservoirs and naturally fractured reservoirs. This chapter reflects some mathematical description in gas coning.

2.2 FLUID FLOW EQUATION

The fluid flow equation assumes the following

- Two dimensional, two-phase incompressible fluid
- Darcy's law apply
- Continuity equation

The radial symmetry equation for both the oil and gas phase is

Oil:

$$\frac{1}{r}\frac{\partial}{\partial r}\left(\frac{rk_h k_{ro}}{\mu_o B_O}\frac{\partial \Phi_O}{\partial r}\right) + \frac{\partial}{\partial z}\left(\frac{k_v k_o}{\mu_o}\frac{\partial \Phi_o}{\partial z}\right) - q_{vo} = \phi\frac{\partial S_O}{\partial t} \quad (1a)$$

Gas

$$\frac{1}{r}\frac{\partial}{\partial r}\left(\frac{rk_h k_{rg}}{\mu_g B_g}\frac{\partial \Phi_g}{\partial r}\right) + \frac{\partial}{\partial z}\left(\frac{k_v kr_o}{\mu_g}\frac{\partial \Phi_o}{\partial z}\right) - q_{vg} = \phi\frac{\partial S_g}{\partial t} \quad (1b)$$

Introducing capillary pressure (Pc) and saturation

$$P_{c_{go}}(S_g) = P_g - P_o = \Phi_g - \Phi_o + z(\gamma_o - \gamma_g) \quad (2)$$

$$S_g + S_o = 1 \quad (3)$$

Equations 1 to 3 forms the basis for the mathematical description has described by some authors in gas coning issues as will be discussed in subsequent sub-section.

2.2.1 DETERMINATION OF CRITICAL RATE, BREAKTHROUGH TIME AND GAS-OIL-RATIO (GOR) PERFORMANCE

2.2.1.1 CRITICAL RATE

Critical rate (Qo) is defines as the maximum allowable oil flow rate that can be imposed on the well to avoid a cone breakthrough. Meyer and Garder (1954) suggest that coning result is as a result of the redial flow of the oil and associated pressure sink around the wellbore.

The critical rate corresponds to the development of a stable cone to an elevation just above the top of the perforated interval in a gas oil system. It depends among other factors, on the vertical permeability of the reservoir, and the distance between the well and the fluid contact surfaces. Other factors that affects critical rate include porosity, anisotropy, reservoir size, horizontal well perforation interval and pressure difference between oil and the coning fluid. It also depends on stand-off and as the stand-off gets smaller with time as the cone grows, the critical rate decreases with time, Muskat (1934).

If a well is produced at a rate of $q_{o,}$right from the gas breakthrough height, h_{gb}, assuming that the height is at $q_{o,}$ then the well will be produced from the gas cap if the production rate is above q_o , and above the gas cap if the rate is below q_o. The critical rate has given in equation – above is thus rearranged to compute for the critical rate in a vertical and horizontal well as follows: for vertical wells

$$q_{co,v} = \frac{k_h h_o^2(\rho_o - \rho_g)}{\mu_o} q_{CD,v} \tag{4}$$

where

$$q_{D,v} = \frac{1.57\times10^{-6}\phi^{0.0113}}{(k_v/k_h)^{0.9477}} \left\{ \frac{1}{\left[\frac{h-h_p-h_{bp}}{h_{gb}+1}\right]^2 - 1} \right\} \left(\frac{1}{1+M^{0.2528}}\right) \frac{(1-\lambda)^{2.5345}}{(1-\varepsilon)^{-2.001}} \tag{5a}$$

$$\delta = \frac{h_p}{h} \tag{5b}$$

$$M = \frac{k_{rg}\mu_o}{\mu_g k_{ro}} \tag{5c}$$

$$\lambda = \frac{h_{bp}}{h} \tag{5d}$$

The height, h_{ob} is calculated when gas breaks into the well for each simulation case. The h_{gb} increases with increase in production rate, oil viscosity etc. For a **horizontal well,** the critical rate is given as:

$$q_{co,h} = \frac{\sqrt{k_h h_o^2} L h_o(\rho_o - \rho_g)}{\mu_o} q_{CD,h} \tag{6}$$

where

$$q_{D,h} = \frac{9.15\times10^{-7}\phi^{1.486}}{(k_v/k_h)^{1.65}}\left\{\frac{1}{\left[\frac{h-h_{bhg}+1}{h_{ahg}+1}\right]^2-1}\right\}\left(\frac{1}{1+M^{0.382}}\right)(1-\lambda)^{2.94} \quad (7a)$$

$$M = \frac{k_{rg}\mu_o}{\mu_g k_{ro}} \quad (7b)$$

$$\lambda = \frac{h_{bhw}}{h} \quad (7c)$$

2.2.1.2 BREAKTHROUGH TIME

Breakthrough time is the time a cone breaks through if the well is producing above its critical rate after a given period of time. Cone breakthrough happens earlier in naturally fractured reservoir due to the presence of fracture system thus lowering the critical rate. Also, production of oil with an economic rate usually causes the breakthrough of cone via fractures into the well and oil will be produced alongside a large amount of gas. Breakthrough time can be determined (in vertical and horizontal wells) as follows: for vertical wells

$$t_{BTV} = 0.2\frac{\phi^{0.913}}{(k_v/k_h)^{0.913}}\left(\frac{1}{q_D}\right)\frac{1}{1+M^{0.214}}(1-\lambda)^{2.296}(1-\varepsilon)^{2.726} \quad (8)$$

and for horizontal wells

$$t_{BTH} = 0.0305\frac{\phi^{1.2013}}{(k_v/k_h)^{0.8819}}\left(\frac{1}{q_D}\right)\frac{1}{1+M^{-0.3119}}(1-\lambda)^{2.8122} \quad (9)$$

2.2.1.3 GOR AFTER BREAKTHROUGH PERFORMANCE

Once gas breakthrough occurs, it's important to predict the performance of gas production as a function of time which is given as: for vertical wells

$$GOR = \left[\left(GOR - Rs_{pwf} + c\right)_{BT}\left(\frac{Np}{Np_{BT}}\right)^m\right] + Rs_{pwf} - c \quad (10)$$

where

c = Constant (20m3/m3)

Constraint of $Np \geq Np_{BT}$

$$m = 0.9377\frac{(k_v/k_h)^{0.0151}(1+M^{0.2324})}{q_D^{0.0513}}(1-\lambda)^{0.4735}m_c^{0.0456} \quad (11a)$$

$$Np_{BT} = q_o \times t_{BT} \quad (11b)$$

$$\left(GOR - Rs_{pwf} + 20\right)_{BT} = \frac{72.0633 q_{D,h}^{0.1787}}{(k_v/k_h)^{0.1233}}(1+M^{0.0557})(1-\lambda)^{0.2791} \quad (11c)$$

and for horizontal wells

$$GOR = \left[\left(GOR - Rs_{pwf}\right)_{BT}\left(\frac{Np}{Np_{BT}}\right)^m\right] + Rs_{pwf} \quad (12)$$

where

Rs_{pwf} varies with the flowing bottom hole pressure, and Np_{BT}, m, and $\left(GOR - Rs_{pwf}\right)_{BT}$ are obtained from regression analysis

$$m = 0.943\frac{(k_v/k_h)^{0.0404}(1+M^{-0.1205})}{q_D^{0.0513}}(1-\lambda)^{0.3326}(1-\varepsilon)^{-0.1558}m_c^{0.0479} \quad (13a)$$

$$Np_{BT} = q_o \times t_{BT} \quad (13b)$$

$$\left(GOR - Rs_{pwf}\right)_{BT} = 3532.12\frac{q_D^{0.7388}(1+M^{0.0341})}{(k_v/k_h)^{0.1233}}(1-\lambda)^{0.3923}(1-\varepsilon)^{4.4694} \quad (13c)$$

2.2.2 MODEL TO PREDICT TWO-PHASE CONING

Coat *et. al.* in their work "numerical simulation of coning using implicit production terms" described a mathematical model to predict two and three phase coning behaviour. They used an analysis of stability with respect to explicit bandling of saturation-dependent transmissibilities to show why explicit transmissibilities can result in a severe timestep restriction for coning simulation.

Equation 1(a) and (b) can be expressed in finite-difference form and solved simultaneously using the iterative alternating discrete technique of Douglas and Rachford. For an incompressible flow in the porous media, equation 1a and b is given for oil and gas as

$$\nabla T_o \nabla \Phi_o - q_o = \frac{vp}{\Delta t}\Delta_t S_o \quad (14a)$$

$$\nabla T_g \nabla \Phi_g - q_g = \frac{vp}{\Delta t}\Delta_t S_g \tag{14b}$$

where

$$\nabla T_o \nabla \Phi_o = \nabla_r T_{ro} \nabla_r \Phi_o + \nabla_z T_{zo} \nabla_z \Phi_o \tag{15a}$$

$$\nabla T_g \nabla \Phi_g = \nabla_r T_{rg} \nabla_r \Phi_g + \nabla_z T_{zg} \nabla_z \Phi_g \tag{15b}$$

and

$$(T_{ro})_{i+1/2,k} = \frac{2\pi\left(\Delta z k_h \frac{k_{ro}}{\mu_o}\right)_{1+1/2,k}}{5.6146 \ln\frac{r_i+1}{r_i}} \tag{16a}$$

$$\left(T_{rg}\right)_{i,k+1/2} = \frac{2\pi\left(\Delta z k_h \frac{k_{rg}}{\mu_g}\right)_{1+1/2,k}}{5.6146 \ln\frac{r_i+1}{r_i}} \tag{16b}$$

$$(T_{zo})_{i,k+1/2} = \frac{2\pi\left(r^2_{i+1/2} - r^2_{i-1/2}\right)}{5.6146} \tag{17a}$$

$$\left(T_{zg}\right)_{i,k+1/2} = \frac{2\pi\left(r^2_{i+1/2} - r^2_{i-1/2}\right)}{5.6146} \tag{17b}$$

The subscripts i and k denote spatial position in the z direction respectively. r_i is radius of the centre of Block i in the radial direction, and $r_{i+1/2}$ and $r_{i-1/2}$ are the radii of the boundaries of Block i in the radial direction. In the simultaneous method of solution, the finite –saturation changes $\Delta_t S_o$ and $\Delta_t S_g$ are expressed in terms of potentials through the use of Eqs. 2.

Determination of saturation changes in terms of potentials for both oil and gas is given as:

$$\Delta_t S_o = S'_g \nabla_t \Phi_o - S'_g \Delta_t \Phi_g \tag{18a}$$

$$\Delta_t S_g = S'_g \nabla_t \Phi_g - S'_g \Delta_t \Phi_o \tag{18b}$$

In Eqs. 16(a) and (b), both the transmissibilities (a flow coefficient in discretization in which when multiply with pressure difference between grid blocks yield flow rate) of $T_{ro}$and T_{rg} and the production term q_g are functions of mobility and functions of saturation. Normally in an incompressible model, the total production rate q for each gridblock is specified and then this production is split among the phases according to their mobilities. That is, for a given producing block, q_g, the production rate of the gas phase is:

$$q_g = q\frac{\lambda_g}{\sum_{i=1}\lambda_i} = q\frac{k_{rg}/\mu_g}{k_{rg}/\mu_g + k_{ro}/\mu_o} \tag{19}$$

2.3 FLUID FLOW EQUATIONS IN DUAL POROSITY MEDIUM

In a fractured reservoir system with two-porosity, two-permeability system, two flow equation is usually described for each of the phase flowing. Most of the fluid occurs in the matrix. Since it has a dual-porosity (a reservoir with two-porosity, two-permeability system normally in a fractured reservoir)model, the matrix will supply fluid to the fracture while the fracture transport or transmit the fluid to the well and as such act as the concept used in the derivation of flow equation for a dual-porosity model. The fluid flow for a two-porosity, two-permeability system is given as:

$$\frac{1}{r}\frac{\partial}{\partial r}\left(\frac{rk_hk_r}{\mu B}\frac{\partial \Phi_O}{\partial r}\right)_f + q'_{mf} = \frac{\partial}{\partial t}\left(\frac{\phi}{B}\right)_f \tag{20a}$$

$$\frac{1}{r}\frac{\partial}{\partial r}\left(\frac{rk_hk_r}{\mu B}\frac{\partial \Phi_O}{\partial r}\right)_m - q'_{mf} = \frac{\partial}{\partial t}\left(\frac{\phi}{B}\right)_m \tag{20b}$$

and the fluid exchange tem is expressed as:

$$-q'_{mf} = \delta\lambda\left(P_m - P_f\right) \tag{21}$$

where

δ and λ are the geometric factor and mobility term respectively.

Chen (1983) introduced a continuous flow in fracture and matrix into the fluid flow equations and assumes that the fluids are immiscible, both the medium and fluids are slightly compressible, and there exists mass transfer between the fracture and matrix so that equation becomes:

$$\nabla\cdot\left(A_{\ell m}\nabla\Phi_{\ell M}\right) - \sigma\lambda_m\left(\Phi_{\ell m} - \Phi_{3-\ell,m}\right) + q_{v\ell m}B_m = \phi_m S_{\ell m}\left(C_{\phi\ell} + C_m\right)\frac{\partial\Phi_{\ell m}}{\partial t} + \phi_\ell\frac{\partial S_{\ell m}}{\partial t} \tag{21}$$

Eq. 2 and 3 for Pressures and saturation can also be rewritten to include matrix and fracture properties as:

$$\Phi_{\ell m} = P_{\ell m} - \gamma_m Z \tag{22}$$

$$S_{\ell 1} + S_{\ell 2} = 1 \tag{23}$$

In Eq. 21,

$$A_{\ell m} = K_{\ell} K_{r\ell m}/\mu_m \tag{24}$$

$$\lambda_m = \frac{K_1 K_{r1m}}{\mu_m} \cdot \frac{K_2 K_{r2m}}{\mu_m} / \left(\frac{K_1 K_{r1m}}{\mu_m} + \frac{K_2 K_{r2m}}{\mu_m} \right) \tag{25}$$

Where

γ = specific weight, Psi/ft.

$S_{\ell 1}$=saturation in fracture

$S_{\ell 2}$= saturation in matrix

Considering the following relations (the simple derivation of the difference equation as presented by Chen *et. al):*

$$\Delta(T^{n+1}\Delta\Phi^{n+1}) = \Delta[(T^n + \Delta_t T)\Delta(\Phi^n + \Delta_t \Phi)] \tag{26}$$

$$= \Delta(T^n \Delta\Phi^n) + \Delta[\Delta T^n \Delta(\Delta_t \Phi)] + \Delta[(T'\Delta_t S)\Delta\Phi^n] \tag{27}$$

and

$$\Delta_t S_{\ell 2} = -\Delta_{\ell} S_{\ell 1} \tag{28}$$

$$\Delta_t \Phi_{\ell 2} = \Delta_{\ell} \Phi_{\ell 1} + P'_{c\ell} \Delta_t S_{\ell 1} \tag{29}$$

Where

$$P'_{c\ell} = P_{\ell 2} - P_{\ell 1} \tag{30}$$

$P'_{c\ell}$= derivative of capillary pressure

$P_{\ell 1}$= derivative of capillary pressure in fracture

$P_{\ell 2}$= derivative of capillary pressure in matrix

Upon substitution into equation 21, equation becomes

$$\Delta_r\{T^n_{r\ell m}\Delta_r[\Delta_t\Phi_{\ell 1}+(m-1)P'_{c\ell}\Delta_t S_{\ell 1}]\}_{ij}+\Delta_z\{T^n_{z\ell m}\Delta_z[\Delta_t\Phi_{\ell 1}+(m-1)P'_{c\ell}\Delta_t S_{\ell 1}]\}_{ij}+\Delta_r\{(T'_{r\ell m}\Delta_t S_{\ell 1})\Delta_r\Phi^n_{\ell m}\}_{ij}+\Delta_z\{(T'_{z\ell m}\Delta_t S_{\ell 1})\Delta_z\cdot\Phi^n_{\ell m}\}_{ij}-\sigma v_{bij}\left(\lambda^n_m+\lambda^n_{\ell m}\Delta_t S_{\ell 1}+\lambda^n_{3-\ell,m}\Delta_t S_{3-\ell,m}\right)_{ij}\cdot\left[\Delta_t\Phi_{\ell 1}-\Delta_t\Phi_{3-\ell,1}+(m-1)\left(P'_{c\ell}\Delta_t S_{\ell 1}-P'_{c,3-\ell}\Delta_t\cdot S_{3-\ell,1}\right)+\Phi^n_{\ell m}-\Phi^n_3-\Phi^n_{3-l,m}\right]_{ij}+q^n_{\ell mij}\left[1+\sum_{u=1}^{J1}\left(\theta^n_{\ell 1iu}cS_{\ell 1iu}+\theta^n_{3-\ell,1iu}\Delta_t S_{3-\ell,1iu}\right)\right]+q'_{\ell mij}\Delta_t S_{\ell 1ij}=\frac{v_{p\ell ij}}{\Delta_t}\left\{S^n_{\ell mij}(C_{\Phi\ell}+C_m)\left[\Delta_t\Phi_{\ell 1ij}+(m-1)P'_{c\ell ij}\Delta_t S_{\ell 1ij}\right]+(3-2m)\Delta_t S_{\ell 1ij}\right\}-\Delta_r\{(T'_{r\ell m}\Delta_r\Phi^n_{\ell m})\}_{ij}-\Delta_z\{(T'_{z\ell m}\Delta_z\Phi^n_{\ell m})\}_{ij} \quad (31)$$

where

$$T_{r\ell m,i-1/2}=\frac{2\pi(\Delta Z)_j K^R_{\ell,i-1/2}K_{r\ell m,i-1/2,j}}{\mu_m ln(r_i/r_{i-1})} \quad (32a)$$

$$T_{z\ell mi,j-1/2}=\frac{2\pi\left(r^2_{i+1/2}-r^2_{i-1/2}\right)_j\left(K^R\right)_{\ell,i-1/2}K_{r\ell m,i-1/2,j}}{\mu_m\left[(\Delta Z)_j+(\Delta Z)_{j-1}\right]} \quad (32b)$$

$$\lambda_{\ell mij}=\lambda^2_{mij}\frac{K'_{r\ell mij}}{\frac{K_{\ell ij}}{\mu_m}K^2_{r\ell mij}} \quad (32c)$$

$$q_{\ell mij}=\frac{B_m K'_{\ell ij}K'_{r\ell mij}q/\mu_m}{\sum_{\mu=1}^{J1}\sum_{\ell=1}^{2}\sum_{m=1}^{2}\frac{K^R_{\ell,iu}K_{r\ell miu}}{\mu_m}} \quad (32d)$$

and

$$\theta_{\ell 1iu}=-\frac{1}{B_1 q}\left(\frac{qK'_r}{K_r}\right)_{\ell 1iu}-\frac{1}{B_2 q}\left(\frac{qK'_r}{K_r}\right)_{\ell iu} \quad (32e)$$

So that if the eq. 31 is expanded by normal expansion and the same variables are merged, the final algebraic equation system to be solved is obtained. The gridblocks are divided so that, in the direction of r, a geometric series scale is used –i.e;

$$r_i=r_i\alpha^{i-1}, i=1,2\ldots.I \quad (33)$$

and satisfies the condition

$$r_e=(r_{I+1}-r_I)/ln(r_{I+1}-r_I) \quad (34)$$

So that radial gridblock scale, α, may be determined by

$$\frac{r_e}{r_1} ln\alpha = \alpha^I - \alpha^{I-1} \tag{35}$$

and in the direction of z, a uniform scale is used.

2.4 CALCULATION OF BREAKTHROUGH TIME IN NATURALLY FRACTURED RESERVOIRS

Al-Afaleg *et. al.* developed a correlation that signifies the influence of matrix and fracture properties on the breakthrough time. The purpose of the correlation was to express the sensitivity of the breakthrough time. In their correlation as presented here, it shows that for homogeneously fractured rock where the major difference between the matrix and fracture control the flow, then the composite effect of reservoir parameters will influence the breakthrough time in a predictable way.

Steps include:

i. Determine dimensionless breakthrough time, t_d

$$t_D = Alog\lambda + B(log\lambda)^2 + C_w + DlogP_{cd} + E\left(\frac{1}{logq_D}\right) + F \tag{36}$$

where

A = -0.051217
B = -0.032583
C =1.557171
D = 0.338711
E = 0.548597
F = 2.493842

$$P_{cd} = \frac{P_c}{\bar{P} - P_{wf}} \tag{37a}$$

$$q_D = \frac{887.31 q_t B_o \mu_o}{k_f h^2 \Delta\gamma} \tag{37b}$$

ii. Determine cumulative oil production at breakthrough, $(N_p)_{BT}$

$$(N_p)_{BT} = \left(\frac{1}{5.615 B_o}\right) A\phi(\overline{S_g} - S_{or})(h - h_{hwb} - h_{ap} - h_p) \tag{38}$$

Where

$$h_{wb} = \frac{h - h_{ap} - h_p}{\sqrt{1 + 39.0633 \times 10^{-4} \left(\frac{1}{r_{De}}\right)^{0.6} \left(\frac{1}{q_{D1}}\right) \left(\frac{1}{1+M^{0.7}}\right) \left(\frac{(1-\varepsilon)^{1.4}}{(1-\delta)^{0.4}}\right)}} \quad (39a)$$

$$r_{De} = r_e/h \quad (39b)$$

$$\varepsilon = h_{ap}/h \quad (39c)$$

$$\delta = h_p/h \quad (39d)$$

$$h_{ap} = h_{oi} - \frac{N_{pres} + G_{pres} + W_{pres}}{A\phi S_g} - h_p - h_{bp} \quad (39e)$$

iii. Determine breakthrough time for homogeneous reservoir, t_{bt1}

$$t_{bt1} = \frac{(N_p)_{BT}}{q_t} \quad (40)$$

iv. breakthrough time t_{bt2} is then calculated for fractured reservoirs as

$$\boldsymbol{t_{bt2} = t_D \times t_{bt1}} \quad \textbf{(41)}$$

The breakthrough time t_{bt1} may be obtained either by simulation studies on an equivalent system, or, a correlation such as the one presented by Weiping and Wattenbarger. The proposed correlation can be used to obtain rough estimates of a correction to the breakthrough time for a given rate for the cone apex in homogeneously reservoir. The steps could be used also to establish a breakthrough time vs. production rate curve for the estimation of critical rate.

3.0 NUMERICAL MODEL

The numerical model used in this work is based on the second technique employed in the numerical methods for the simulation of well coning behaviour as described by Coats *et. al*. The second model technique employs the implicit pressure- explicit saturation (IMPES) analysis with production term treated explicitly while the interblock transmissibilities are treated implicitly in the saturation equation. The model is improved to include fracture and matrix properties. IMPES is applied to discretization of the diffusivity equations and uses a time level of '$t + \Delta t$' in Taylor's series expansion.

3.1 DESCRIPTION OF THE CONING MODEL

IMPES analysis is applied to the difference equations that describe two-phase (oil and gas) flow in a cylindrical geometry of a homogeneous fractured reservoir. The terms involving saturation change over a given time step is eliminated by combining with the original difference equations. The saturation dependent terms (transmissibilities and capillary pressure) which remain in the potential equation as coefficients or constants is treated explicitly. The fact that the capillary pressure is treated explicitly in the potential equation is sufficient to cause conditional stability (i.e. a time-step restriction). After the potential equation distribution has been computed from the potential equation, the saturations are updated directly from the original difference equations. In the calculation, the individual oil or gas production rate are saturation dependent and are treated implicitly as $q_{gn} + q'_g \Delta_t S$ where q_{gn} is the change in gas flow rate with saturation change.

To preserve the simplicity of the IMPES technique, the transmissibility still is treated explicitly in the potential solution portion of the model. Saturation distribution is calculated using implicit transmissibilities. Since transmissibilities are interblock, saturation dependent properties, their values depend not only on the fluid saturation in the adjacent blocks. Substituting the implicit transmissibility expression into the saturation equation results in a system of equations which may again be solved by Gaussian elimination technique. The model has significant features in that only in the near-well region of the grid in the implicit treatment of the transmissibility is necessary so that the explicitly calculation of saturation changes can be used elsewhere in the grid system. The explicit treatment of the capillary pressure in the potential equation is sufficient to limit the size of the maximum stable time step.

3.2 MATHEMATICAL DESCRIPTION OF THE MODEL

Recalling the fluid-flow equation in chapter 2 as:

$$\frac{1}{r}\frac{\partial}{\partial r}\left(\frac{rk_h k_{ro}}{\mu_o B_O}\frac{\partial \Phi_O}{\partial r}\right) + \frac{\partial}{\partial z}\left(\frac{k_v k_o}{\mu_o}\frac{\partial \Phi_o}{\partial z}\right) - B_o q_{vo} = \phi \frac{\partial S_O}{\partial t} \quad (1a)$$

$$\frac{1}{r}\frac{\partial}{\partial r}\left(\frac{rk_h k_{rg}}{\mu_g B_g}\frac{\partial \Phi_g}{\partial r}\right) + \frac{\partial}{\partial z}\left(\frac{k_v kr_o}{\mu_g}\frac{\partial \Phi_o}{\partial z}\right) - B_g q_{vg} = \phi \frac{\partial S_g}{\partial t} \quad (1b)$$

where the potential are defined as

$$\Phi_o = P_o - \gamma_o z$$

$$\Phi_g = P_g - \gamma_g z$$

and the pressures in each fluid phase can be related by capillary pressure (equation below) which is taken as a function of gas saturation alone.

$$P_{c_{go}}(S_g) = P_g - P_o = \Phi_g - \Phi_o + z(\gamma_o - \gamma_g) \quad (2)$$

The saturations in each phase sum to unity as

$$S_g + S_o = 1 \quad (3)$$

Equation 1(a) and (b) can be expressed in finite-difference form as in eq. 5

$$\Delta(T_o \Delta\Phi_o)_{i,j} - q_{o_{i,j}} = \frac{V_{p_{i,j}}}{\Delta t}\left(S_{o_{n+1}} - S_{o_n}\right)_{i,j} \quad (42a)$$

$$\Delta\left(T_g \Delta\Phi_g\right)_{i,j} - q_{g_{i,j}} = \frac{V_{p_{i,j}}}{\Delta t}\left(S_{g_{n+1}} - S_{g_n}\right)_{i,j} \quad (42b)$$

where

$$\Delta(T_o \Delta\Phi_o) = \Delta_r(T_{ro}\Delta_r\Phi_o) + \Delta_z(T_{zo}\Delta_z\Phi_o) \quad (43)$$

$$q_{o_{i,j}} = B_o q_{vo} q_{vo_{i,j}} \quad (44)$$

The coefficients of the pressure difference are obtained as transmissibilities. In the radial direction,

$$(T_{ro})_{i-1/2,j} \equiv \frac{2\pi(\Delta Z)\left(\frac{k_h k_{ro}}{\mu_o}\right)_{1-1/2,j}}{\mu_o \ln\frac{r_i}{r_{i-1}}} \quad (45a)$$

and in the vertical direction

$$(T_{ro})_{i,j-1/2} \equiv \frac{2\pi\left(r_{i+1/2}^2 - r_{i-1/2}^2\right)_i (K_z K_{ro})_{1,j-1/2}}{\mu_o\left[(\Delta Z)_j + (\Delta Z)_{j-1}\right]} \quad (45b)$$

For a block-centred radii $r_i, i = 1, I, i$

$$r_i = \alpha^{i-1} r_1 \quad (33)$$

and satisfies the condition

$$r_e = (r_{I+1} - r_I)/ln(r_{I+1} - r_I) \quad (34)$$

α is chosen so that the exterior radius is the log-mean between r_I and r_{I+1}. The block boundary radii r_{I+1} are the log-mean radii

$$r_{i+1/2} = \frac{(r_{i+1} - r_I)}{ln\frac{r_{i+1}}{r_i}} \quad (46)$$

The IMPES method is probably the most direct technique for solving the simultaneous two-phase fluid flow equation. First step is the elimination of the saturation variable. When eq. 42a and 42b are added together, the sum of the terms on the right-hand side of the equation is zero since the total saturation most be $(S_g + S_o)$ unity, i.e.

$$\Delta(T_o \Delta\Phi_o)_{i,j} + \Delta\left(T_g \nabla\Phi_g\right)_{i,j} - \left(q_o + \mathrm{q}_w\right)_{i,j} = 0 \quad (47)$$

where the production term is now the total fluid production rate from the gridblock which is designated as:

$$\boldsymbol{q_{i,j}} = \boldsymbol{q_{o_{i,j}}} + \boldsymbol{q_{g_{i,j}}} \quad (48)$$

The relative amounts of oil and gas production is computed from the saturation-dependent mobilities of the two fluids in the production gridblock.

Equation 42 can be written in terms of a single potential in the form,

$$\Delta\left(T\Delta\Phi_g\right)_{i,j} = B_{i,j} \quad (49)$$

All saturation-dependent terms (transmissibilities and pressure) are taken at the previous time step. The implicit gas production from the gridblock may be expressed as:

$$q_{g_{n+1}} = q_{g_n} + qf'\left(S_{g_{n+1}} - S_{g_n}\right) \quad (50)$$

where

$$f' = \frac{\left(f_{g_{n+1}} - f_{g_n}\right)}{\left(S_{g_{n+1}} - S_{g_n}\right)}$$

Replacing the n-level gas production term in eq. 40a and 40b by the implicit gas production term in eq. above, we have

$$\boldsymbol{S_{g_{n+1}}} = \boldsymbol{S_{g_n}} + \frac{\left[\Delta\left(\boldsymbol{T_g}\Delta\Phi_g\right)_{i,j} - \boldsymbol{q_g}\right]_{i,j}}{\left(\frac{\boldsymbol{V_p}}{\Delta \boldsymbol{t}} + \boldsymbol{q f'}\right)_{i,j}} \tag{51}$$

To now introduce transmissibilities in the gridblock near the wellbore following the implicit production processes then we need to consider the potential given in eq. 51. The transmissibilities enter into the pressure solution, whereas in the source term, only the total production rate is needed rather than the separate oil or gas production rates. The transmissibilities are treated explicitly in the potential equation to preserve the complicity of the IMPES analysis. Saturation calculation is examined by expanding eq. 51 by neglecting the effect of implicit transmissibilities on the pressure solution.

The transmissibilities and oil production rates in terms of the $n+1$ time level is expressed as

$$\Delta\left(T_{g_{n+1}}\Delta\Phi_{g_n}\right)_{i,j} - q_{g_{i,j,n+1}} = \frac{V_p}{\Delta t}\left(S_{g_{n+1}} - S_{g_n}\right)_{i,j} \tag{52}$$

Transmissibilities at the $n+1$ time level is expressed as

$$T_{g_{i,j,n+1}} = A_{g_{i,j,}}\left[(1-w)K_{rg_{i,j,n+1}} + K_{rg_{i-1,j,n+1}}\right] \tag{53}$$

where $A_{g_{i,j,}}$ contains non-saturation dependent terms in the transmissibilities definition. The values $K_{g_{n+1}}$ can be approximated by

$$K_{rg_{n+1}} = K_{rg_n} + K'\left(S_{g_{n+1}} - S_{g_n}\right) \tag{54}$$

where

$$K' \equiv \frac{K_{rg_{n+1}} = K_{rg_n}}{\left(S_{g_{n+1}} - S_{gn}\right)} \tag{55}$$

combining eq. 54 and 55 yields

$$T_{g_{i,j,n+1}} = T_{g_{i,j,n}} + A_{g_{i,j}}\left[(1-w)K'_{i,j}(\Delta_t S)_{i,j} + wK'_{i-1,j}(\Delta_t S)_{i+1,j}\right] \quad (56)$$

where

$$\Delta_t S = S_{g_{n+1}} - S_{g_n} \quad (57)$$

$w =$ Weighting factor and is taken to be 0 or 1 to wright relative permeability upstream.

Substituting eq. 56 into 50 gives the new saturations in the designated implicit transmissibilities region as:

$$\boldsymbol{C_{i+1,j}}(\Delta_t \boldsymbol{S})_{\boldsymbol{i+1,j}} - \boldsymbol{D_{i,j}}(\Delta_t \boldsymbol{S})_{\boldsymbol{i-1,j}} + \boldsymbol{E_{i,j}}(\Delta_t \boldsymbol{S})_{\boldsymbol{i,j+1}} - \boldsymbol{F_{i,j}}(\Delta_t \boldsymbol{S})_{\boldsymbol{i,j-1}} + \boldsymbol{G_{i,j}}(\Delta_t \boldsymbol{S})_{\boldsymbol{i,j}} = \boldsymbol{H_{i,j}} \quad \textbf{(58)}$$

Where C, D, etc., are expressions involving transmissibility-pressure difference terms. The number of grid blocks in which the transmissibilities are treated implicitly may be limited to those near the wellbore. However, the equation is used to compute new saturations in the designated implicit transmissibility region while eq. 51 is employed over the rest of the grid.

4.0 CONSTRUCTING THE SIMULATION MODEL

4.1 SIMULATION MODEL DESCRIPTION

The numerical simulation is performed using a single well radial model and a fracture-matrix model in Eclipse simulator.

4.1.1 SINGLE WELL RADIAL MODEL

The reservoir is initially at capillary/gravity equilibrium of 3,600 psia (24.8 MPa) at the gas/oil contact depth of 9,035 ft (2754 m). The reference capillary pressure at the contact is 0 psi. The single production well at the center of the well is completed in Blocks 1, 7 and 1, 8 as shown in fig 4.1.

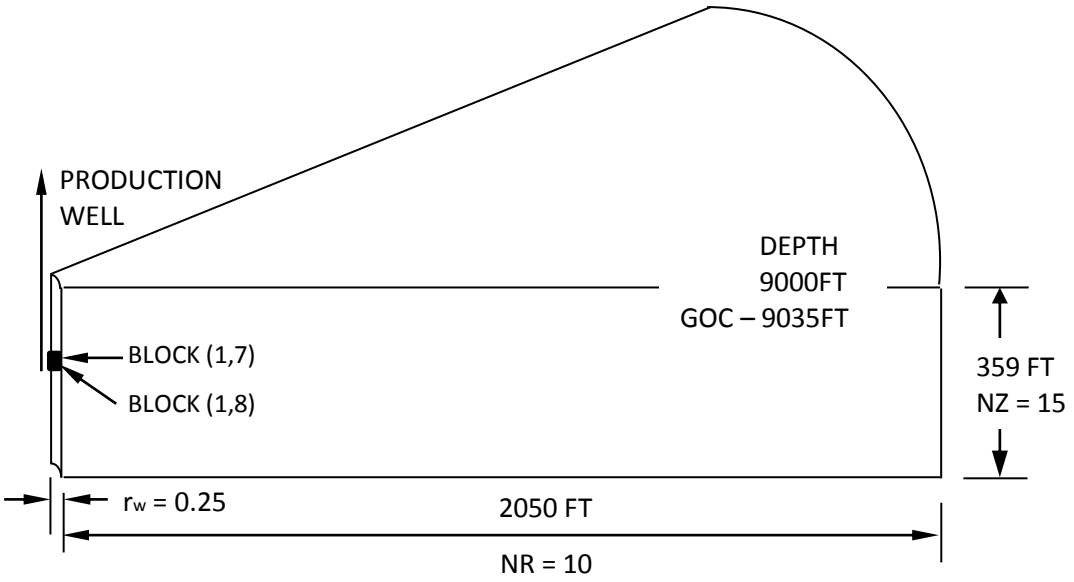

Figure 4.1: Reservoir Model

The well name is 'P1' and is a single radial well that is connected to two grid blocks. The numbers of radial block considered is 10 with 15 numbers of vertical layers having different porosity value, anisotropy ratio, and thickness considered as the oil pay zone (table 4.1). A Permeability-thickness of 6200md-ft and 480md-ft is used for the completion in block 1,7 and 1,8 respectively. Rock and fluid properties presented in tables 4.1 to 4.4 are commonly used in simulation studies. Reservoir properties and stratification are detailed in table 4.1.
As simulation is in progress, only a small fraction of the total number of gridblock will probably experience sufficient large surges in pressure and/or saturation to justify implicit treatment. As simulation proceeds, cells requiring implicit treatment will change. Since coning is a well phenomenon and not a gross reservoir phenomenon, the grid blocks must

necessary be small in the vicinity of the wellbore because both pressures and saturations vary rapidly in this region. The well is located at the linear boundary of each gridblock and the production schedule is to be maintained until the BHFP is equal to the constraint value.

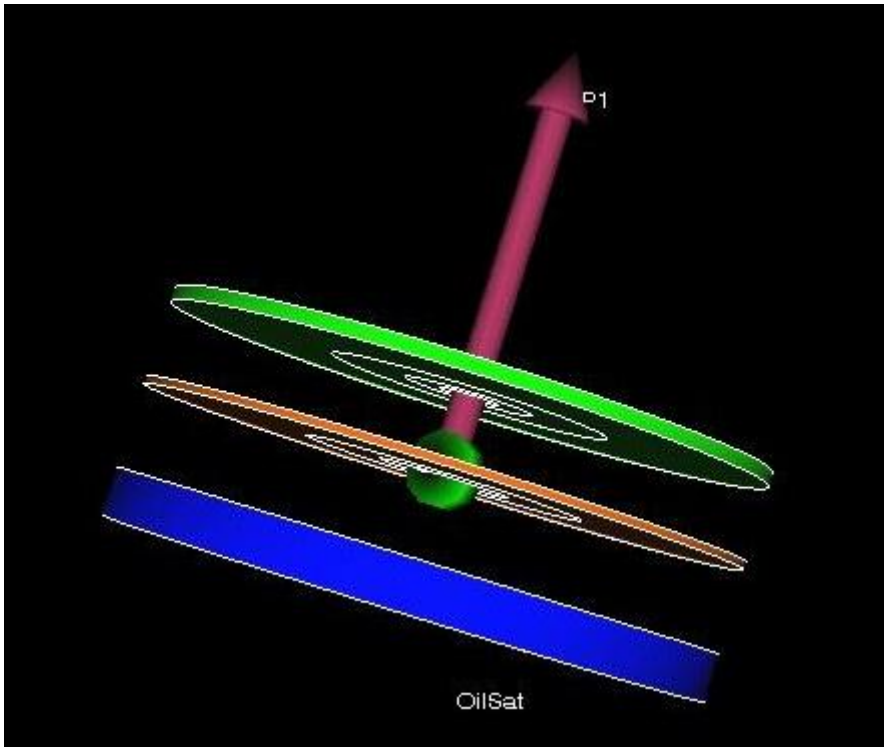

Figure 4.2: well connection at the center of the radial system completed in Blocks 1,7 and 1,8

Layer	**Thickness** (ft)	K_x (md)	K_z (md)	**Porosity**
1	20	35	3.5	0.087
2	15	47.5	4.75	0.097
3	26	148	14.8	0.111
4	15	202	20.2	0.16
5	16	90	9	130
6	14	418	41.8	0.17
7	**8**	**775**	**77.5**	**0.17**
8	**8**	**60**	**6**	**0.08**
9	18	682	68.2	0.14
10	12	472	47.2	0.13
11	19	125	12.5	0.12
12	18	300	30	0.105
13	20	137	13.7	0.12
14	50	191	19.1	0.116
15	100	350	35	0.157

Table 4.1: Reservoir Description

4.1.2 FRACTURE AND MATRIX MODEL

A dual-porosity, single-permeability system is used since matrix blocks are linked only through the fracture system i.e. Fluid flow through the reservoir takes place only in the fracture network with the matrix block acting as the source. The model has the shape of a cube. The keyword DUALPORO is specified in the RUNSPEC section thus the number of layers entered in item 3 of the DIMENS keyword of the data file is even. ECLIPSE interprets the first half of the grid layers as a matrix cells, and the remainder as fracture cells and the non-neighbour connections representing matrix-fracture flow transmissibilities are automatically constructed.

Gas-oil gravity drainage mechanism is considered as the mechanism since the fluid exchange is between the fracture and matrix due to gravity. The gravity drainage method used is a discrete Matrix model (E100) that uses *N* matrix porosities (where *N* is user-defined to create a vertical stack of finely spaced matrix cells which describe the distribution of properties within the single block of matrix material and the height is defined using the keyword DZMTRZ)

The geometry of the grid cells representing the models are defined in Cartesian coordinates. Each grid cell in the model is defined in the simulator to be either matrix or fracture. The "unit block'' is a 1.0ft high cubical matrix block with a diameter of 1.0ft. The blocks are separated by a horizontal fracture of 0.01ft. Matrix contact between the blocks in the stack is established by defining the grid cell in the separating fractures as matrix. The radius of the grid cell is changed to vary the area of contact between the blocks. The ''unit'' block is divided into 6 grid cells in the X-direction, 6 grid cells in the Z-direction and 1 grid cell in the Y-direction. The grid cell representation is equal in all "unit'' block used in the model. The injector is placed at the top of the grid cell (1,1) and the producer at the bottom in the grid cell (6,6).

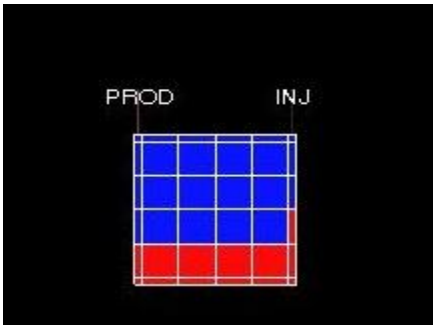

Figure 4.3: Simulated model of a single block

4.1.2.1 FRACTURE PROPERTIES

The fracture is modelled in the simulator as a matrix rock with 100% porosity and the physical characteristics of the fracture is formulated in terms of matrix block properties so as to serve as input to the simulator. Figure 4.4 shows a single producing well model configured with fracture network. The role of the fracture is to supply sufficient volume of gas to the matrix to maintain displacement process. The fractures are initially saturated with gas. The matrix and fractures are such that the input matrix permeability curves for the fractures will have no significant effect on results obtained.

4.2 RESERVOIR FLUID AND ROCK PROPERTIES

The oil and gas phase are inert. No gas is liberated or dissolved in the oil. Reservoir pressure, temperature and pvt properties of the oil and gas are given values that could be expected in any reservoir. Tables 4.2 display the PVT properties.

4.2.1 RELATIVE PERMEABILITIES

Permeability is the ability of a rock to transmit fluids, and it can be refer to 100% saturation of single – phase fluid, designated with the symbol k. here, the rock is saturated with only gas and oil fluid. However, permeability defers between the absolute, effective, and relative permeability. While the absolute permeability measures the permeability when a single fluid or phase is present in the rock, the effective permeability describes the simultaneous flow of more than one fluid i.e. it has the ability to preferentially flow or transmit fluid through a rock when the other immiscible fluids are present in the reservoir. Relative permeability is the ratio of effective permeability of a given phase (fluid) at a particular saturation, to the absolute permeability of that phase (fluid) at a total saturation.

$$k_{ro} = \frac{k_o}{k} \tag{59}$$

Where

k_{ro} = relative permeability of oil

k_o = permeability of oil

k_o = absolute permeability of oil

The relative permeabilities are influenced by the following factors; saturation, saturation history, wettability, temperature, viscous, capillary and gravitational forces. Values used are given in table 4.3.

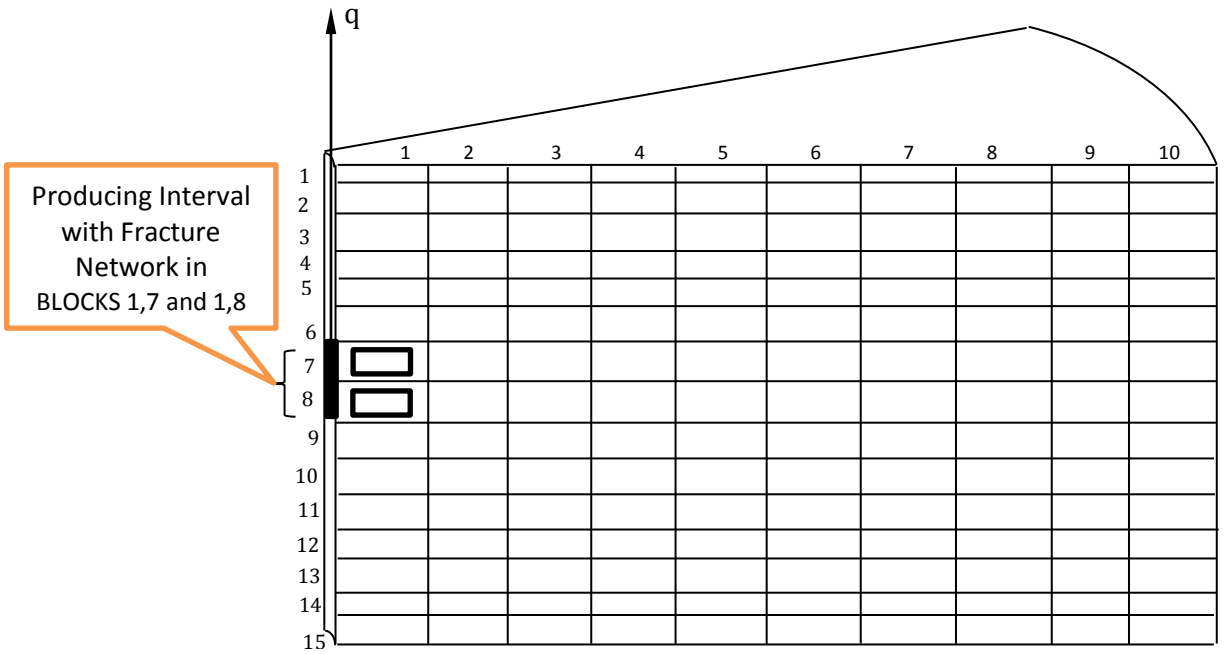

Figure 4.4: configured reservoir around a single producing well in a homogeneous fractured reservoir

	Saturated Oil				gas		
Pressure (psia)	B_o (RB/STB)	Density (lbm/cuft)	μ (cp)	Solution GOR (scf/STB)	B_g (Mcf/STB)	Density (lbm/cuft)	μ (cp)
400	1.0120	49.497	1.17	165	5.90	2.119	0.0130
800	1.0255	48.100	1.14	335	2.95	4.238	0.0135
1200	1.0380	49.372	1.11	500	1.96	6.397	0.0140
1600	1.0510	50.726	1.08	665	1.47	8.506	0.0145
2000	1.0630	52.072	1.06	828	1.18	10.596	0.0150
2400	1.0750	53.318	1.03	985	0.98	12.758	0.0155
2800	1.0870	54.399	1.00	1,130	0.84	14.885	0.0160
3200	1.0985	55.424	0.98	1,270	0.74	16.896	0.0165
3600	1.1100	56.203	0.95	1,390	0.65	19.236	0.0170
4000	1.1200	56.930	0.94	1,500	0.59	21.192	0.0175
4200	1.1300	57.534	0.92	1,600	0.54	23.154	0.0180
4600	1.1400	57.864	0.91	1,676	0.49	25.517	0.0185
5200	1.1480	58.267	0.90	1,750	0.45	27.785	0.0190
5600	1.1550	58.564	0.89	1,810	0.42	29.769	0.0195

Table 4.2: PVT Properties

4.2.1.1 RELATIVE PERMEABILITY CURVE

Relative permeability curve has great influence on the gas coning and also on matrix – fracture properties. In the matrix it is assumed that only drainage displacement process will occur, so the constructed curves (fig. 4.5) will represent drainage conditions were gas displaces oil imbibition condition.

The curve contains element such as: the end point fluid saturations; the end point permeabilities and the curvature of the relative permeability. The end point saturations determine the range of the movable saturation and are directly related to amount of recoverable oil that can be obtained. The end points of relative permeabilities account for the mobility ratio and will determine sweep efficiency of a displacement process. The shape of the curve in between may also have an important bearing on recovery efficiency. Since a gas-oil system is considered, gas will be displacing oil that completely fills the porous rock. Only drainage curve is required. The shape of the curves depends on the surface tension of the system, as well as on the rock characteristics.

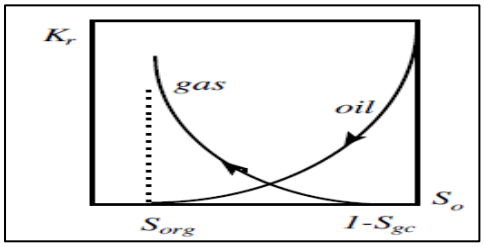

Figure 4.5: typical curve for oil-gas relative permeability

4.2.1.2 TWO-PHASE RELATIVE PERMEABILITY MODEL

For a two phase (oil- gas system), the Corey's model correlation is used to determine table 4.4 which is then used to produce fig. 4.6.

$$k_{ro} = k'_{ro}\left[\frac{s_o - s_{or}}{1 - s_{or} - s_{gir}}\right]^{\lambda} \quad (60)$$

$$k_{rg} = k'_{rg}\left[\frac{s_g - s_{gir}}{1 - s_{or} - s_{gir}}\right]^{\lambda} \quad (61)$$

where

$\left[\frac{s_o - s_{or}}{1 - s_{or} - s_{gir}}\right] = s_o^*$ = normalized oil saturation

$\left[\frac{s_g - s_{gir}}{1 - s_{or} - s_{gir}}\right] = s_g^*$ = normalized gas saturation

4.2.2 CAPILLARY PRESSURE CURVE

Capillary pressure curve is constructed so that the capillary forces will play significant role in the drainage process as presented in fig. 4.11

4.2.3 RESIDUAL OIL SATURATION

Connate water does not take part in the production process but its presence in the pores influence indirectly on the relative permeability of the residual oil saturation and even relative permeability. The residual oil or liquid saturation is 0.30.

Geometry	
Radial extent, ft	2,050
Wellbore radius, ft	0.25
Radial position of first block centre, ft	0.84
Number of radial blocks	0.25, 2.00, 4.32, 9.33, 20.17
Number of vertical layers	15
Dip angle, degrees	0
Depth to top of formation, ft	9,000
Radial block boundaries, ft	0.25, 2.00, 4.32, 9.33, 20.17, 43.56, 94.11, 203.32, 439.24, 948.92, and 2,050.00
Rock and Fluid Data	
Pore compressibility, psi^{-1}	4×10^{-6}
Water compressibility, psi^{-1}	3×10^{-6}
Oil compressibility for undersaturated oil, psi^{-1}	1×10^{-6}
Oil viscosity compressibility for undersaturated oil, psi^{-1}	0
Stock-tank oil density, Ibm/cu ft	45.0
Stock-tank water density, Ibm/cu ft	63.02
Standard-condition gas density, Ibm/cu ft	0.0702
Initial Conditions	
Depth of gas/oil contact, ft	9,035
Oil pressure at gas/oil contact, psi	3,600
Capillary pressure at gas/oil contact, psi	0
Depth of water/oil contact, psi	9,209
Capillary pressure at water/oil contact, psi	0
Well Data	
Completed in blocks	(1,7) (1,8)
Permeability thickness	6,200 480
Skin	0 0
Minimum BHFP	3,000
Pump depth, ft	9,110

Table 4.3: Basic Data

Sg	Krg	Pcog
0.0000	0.0000	0.0069
0.1000	0.0183	0.0103
0.2000	0.0835	0.0152
0.3000	0.1692	0.0221
0.4000	0.2695	0.0345
0.5000	0.3815	0.0531
0.6000	0.5036	0.0793
0.7000	0.6345	0.1324
	fracture	
0.0000	0.0000	0.0000
1.0000	1.0000	0.0000

Table 4.4: relative permeability and capillary pressure data

4.3 BASIC FLOW EQUATIONS

The fluid flow for a two-porosity, two-permeability system is given as:

$$\frac{1}{r}\frac{\partial}{\partial r}\left(\frac{rk_h k_r}{\mu B}\frac{\partial \Phi_O}{\partial r}\right)_f + q'_{mf} = \frac{\partial}{\partial t}\left(\frac{\phi}{B}\right)_f \tag{20a}$$

$$\frac{1}{r}\frac{\partial}{\partial r}\left(\frac{rk_h k_r}{\mu B}\frac{\partial \Phi_O}{\partial r}\right)_m - q'_{mf} = \frac{\partial}{\partial t}\left(\frac{\phi}{B}\right)_m \tag{20b}$$

and the fluid exchange tem is expressed as:

$$-q'_{mf} = \delta\lambda\left(P_m - P_f\right) \tag{21}$$

Then, for a continuous flow of fluid in the fracture and matrix, the flow of fluid will satisfy the following equation:

$$\nabla\cdot\left(A_{\ell m}\nabla\Phi_{\ell M}\right) - \sigma\lambda_m\left(\Phi_{\ell m} - \Phi_{3-\ell,m}\right) + q_{v\ell m}B_m = \phi_m S_{\ell m}\left(C_{\phi\ell} + C_m\right)\frac{\partial\Phi_{\ell m}}{\partial t} + \phi_\ell\frac{\partial S_{\ell m}}{\partial t} \tag{21}$$

Eq. 2 and 3 for Pressures and saturation can also be rewritten to include matrix and fracture properties as:

$$\Phi_{\ell m} = P_{\ell m} - \gamma_m Z \tag{22}$$

$$S_{\ell 1} + S_{\ell 2} = 1 \tag{23}$$

In Eq. 21,

$$A_{\ell m} = K_{\ell} K_{r\ell m} / \mu_m \tag{24}$$

$$\lambda_m = \frac{K_1 K_{r1m}}{\mu_m} \cdot \frac{K_2 K_{r2m}}{\mu_m} \Big/ \left(\frac{K_1 K_{r1m}}{\mu_m} + \frac{K_2 K_{r2m}}{\mu_m} \right) \tag{25}$$

Where

$S_{\ell 1}$=saturation in fracture

$S_{\ell 2}$= saturation in matrix

i, j = gridblock indices in r and z directions

ℓ = 1 for fracture; and 2 for matrix

m = 1 for gas; 2 for oil; with numerical errors being introduced by the timestep procedure, the convergence acceleration, and roundoff with total error estimated between 4 to 10%.

4.3.1 INITIAL AND BOUNDARY CONDITIONS

Both the two phase fluid (oil and gas) present in the reservoir is at a capillary/equilibrium before the well in put into production at a schedule production rate of with a reference pressure of 3600psia with a Gas-Oil Contact (GOC) at a depth of 9,035ft (2754m). Due to the combined action of the capillary and gravity, the oil potential is kept constant since water is not considered (no transition zone between oil and water). The reference capillary pressure at each contact is 0psi. Initial gas saturation, S_g, is obtained by the capillary pressure/saturation relationship for fracture and matrix, fig. 4.5 and 4.7. Production rate at perforated interval 1,7 and 1,8 is specified. The mobility ratio and total fluid production rate determines gas and oil percentage production. There is no flow across boundaries of cylinders. As stated in section 4.1.2, the ‘‘unit’’ block is divided into 6 grid cells in the X-direction, 6 grid cells in the Z-direction and 1 grid cell in the Y-direction. The grid cell representation is equal in all “unit’’ block used in the model. The injector is placed at the top of the grid cell (1,1) and the producer at the bottom in the grid cell (6,6). The well is located at the linear boundary of each gridblock and the production schedule is to be maintained until the BHFP is equal to the constraint value.

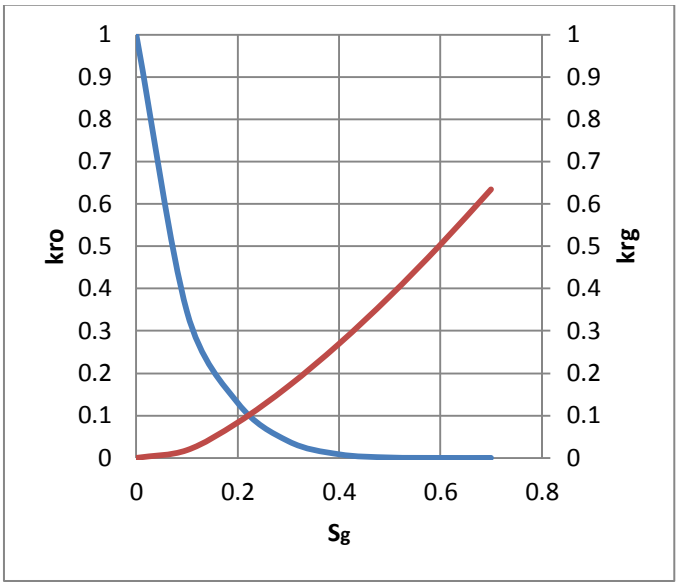

Figure 4.6: Gas-oil relative permeability curve

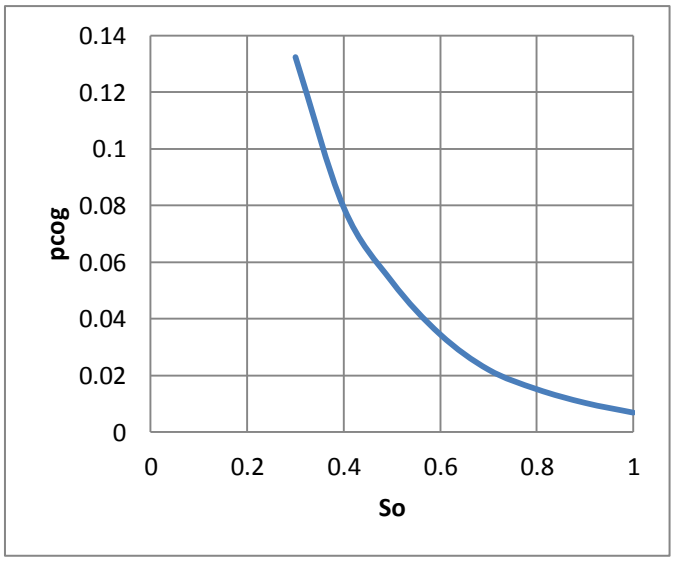

Figure 4.7: Drainage capillary pressure curve

4.4 SENSITIVITY STUDIES

A reservoir simulation study has previously being performed to understand the effect of fracture and matrix properties on gas production behaviour in a naturally fractured reservoir. As a further study, a parametric study is conducted to investigate and analyse the effect of fracture parameters on gas coning phenomena in a naturally fractured reservoir. Parameters to investigate will include oil flow rate, matrix and fracture porosities, horizontal and vertical permeabilities in matrix and fractures, fracture spacing, matrix block size, mobility ratio, vertical to horizontal permeability ratio (anisotropy ratio), oil reservoir

thickness, oil and gas densities etc. Figs. 4.8a to 4.8d show the initial result before fracture and matrix presence. Fig. 4.9 depicts inclusion of fracture and matrix; results are presented in the next chapter.

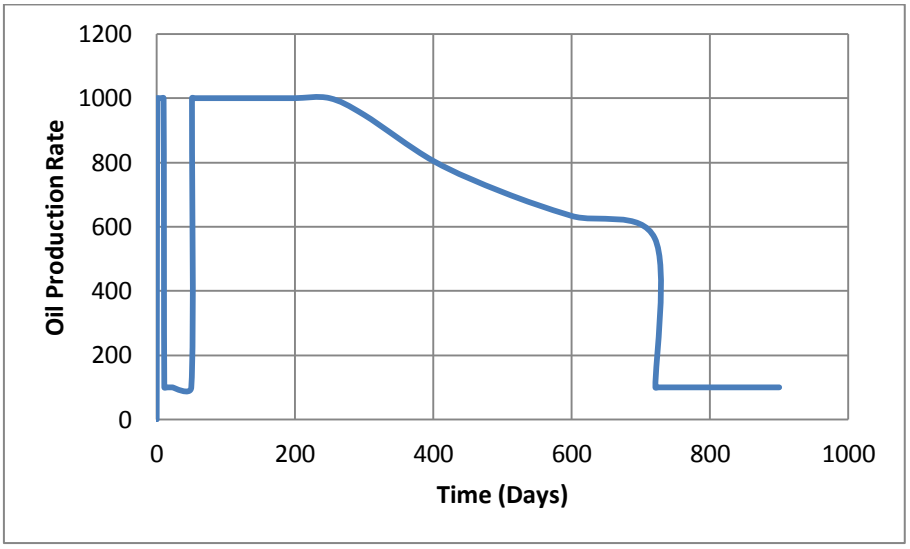

Figure 4.8(a): Production rate vs. Time

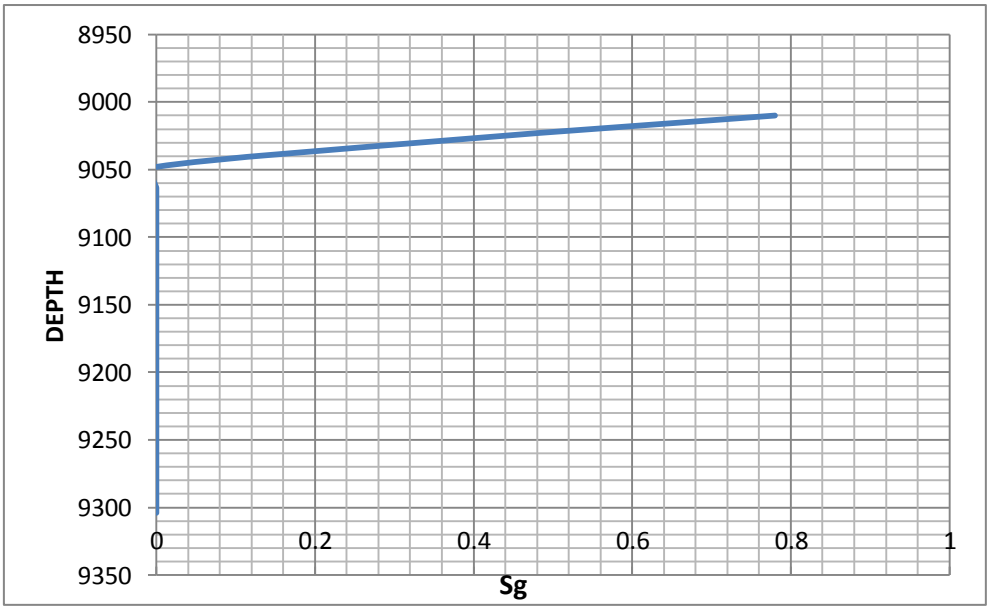

Figure 4.8(b): Depth vs. Saturation

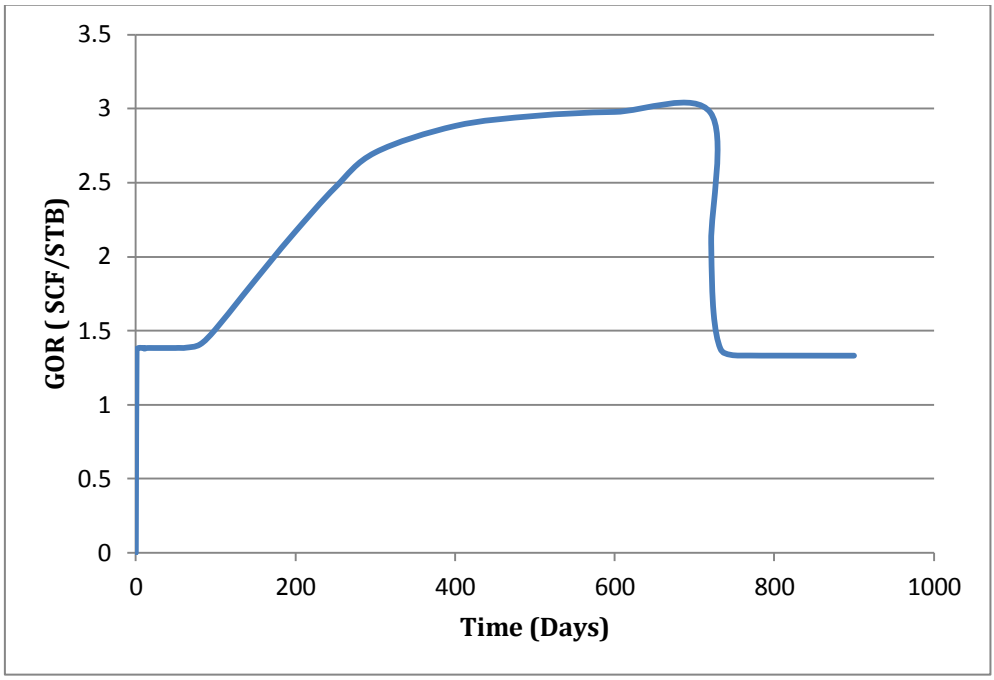

Figure 4.8(c): GOR vs. Time

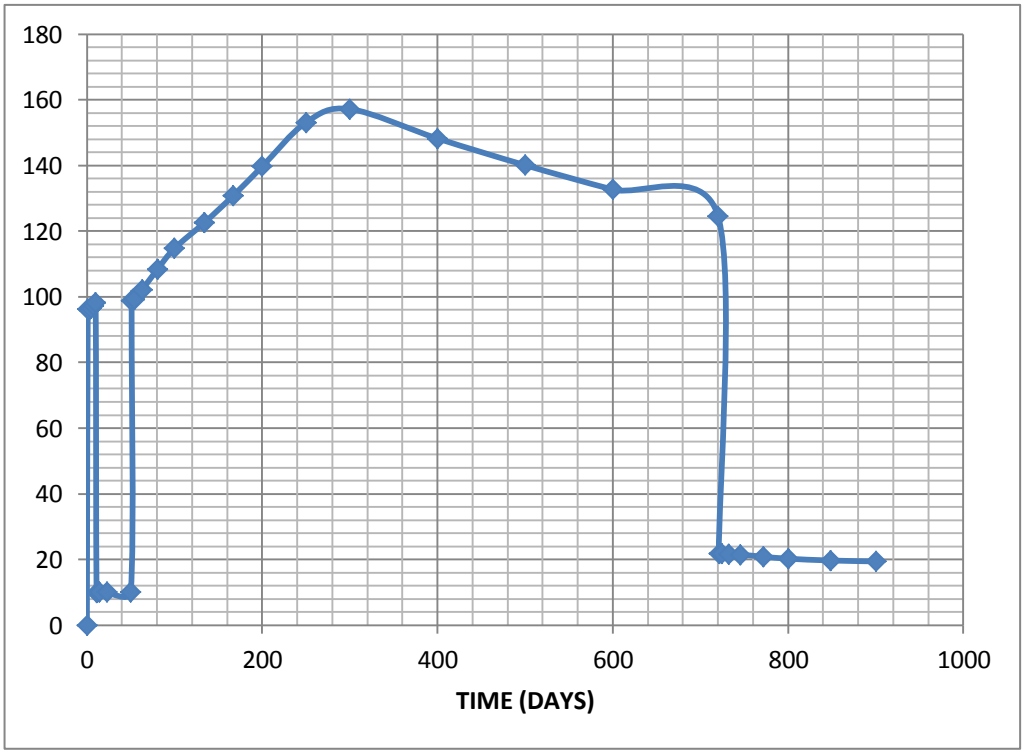

Figure 4.8(d): Pressure Drawdown vs. Time

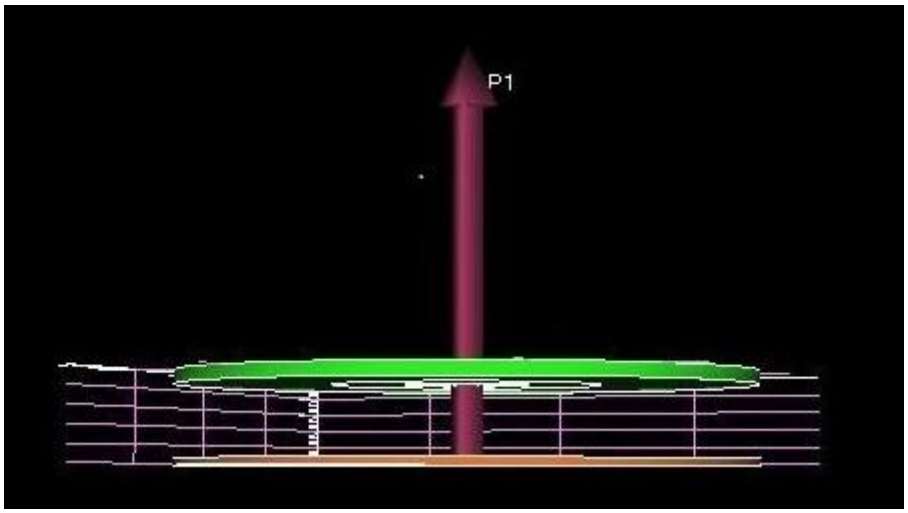

Figure 4.9: Matrix and Fracture properties included in Blocks 1,7 and 1,8

5.0 SENSITIVITY ANALYSIS (RESULTS AND DISCUSSION)

Several simulation runs have being performed to investigate effective parameters of gas coning of a single radial well in a naturally fractured reservoir. A base case was set-up by modelling matrix and fracture properties using the Chappelear 3 phase radial coning study data file. Thereafter, eleven different parameters were varied for the sensitivity analysis to compare with the base case which resulted in 32 simulation runs and the results are shown in figs. 5.1 to 5.13. With the understanding of fracture patterns around the producing well, matrix and fractures is modelled which generates **fig. 5.1** which compares the initial data file before the inclusion of the matrix and fracture properties. In the fig. 5.1, due to the presence of fracture system in a naturally fractured reservoir, gas breakthrough tends to occur earlier which also reduces the critical production rate. If the oil is produced at an economic rate it will cause the cone to breakthrough via the fractures into the well thereby producing oil alongside gas. The gas produced alongside oil causes reduction of oil production making the well uneconomical.

Fig. 5.2 depicts oil production rate effect where five cases were run by varying the flow rate which as shown in the figure the higher the flow rate the earlier the cone breakthrough will occur. The highest flow rate of 3000stb/day used in the simulation run resulted to an earlier breakthrough at 38 days, while the lowest flow rate of 600 stb/day delays coning till 200days. GOR after breakthrough time slightly increases when production rate is increased and slightly reduces when production rate is lowered. **Table 5.1** shows the cumulative oil and gas production until gas breakthrough with cumulative oil production highest at 630,000 bbls when 3000 stb/day flow rate is considered compare to the base case of 1000stb/day resulting in a cumulative oil production of 624,000 bbls with breakthrough time occurring at 65 days. However, the increase in flow rate increases oil production rate and accelerates the recovery. Influence of gas breakthrough time is shown in **fig. 5.3.**

Fig. 5.4 shows matrix and fracture porosity effect. If the matrix porosity is increased, fracture porosity is reduced and vice versa, there seems to be no influence on breakthrough time and GOR. In the plots, the base case matrix fracture is 0.3 ft. and the fracture porosity is 1.0 ft, a further increase of matrix and fracture porosity of 0.6 and 1.3 is used respectively, and also a reduction in matrix and fracture of 0.03 and 0.1 was varied to ascertain how porosity affects GOR. However, at the end of the run, a reduced matrix and fracture porosity results in earlier breakthrough time of 60 days and subsequently increases GOR after breakthrough while an increase in matrix and fracture porosity though have a longer breakthrough time at 82 days, reduces GOR after breakthrough time compared to base case of 65 days

breakthrough time. Increase in matrix and fracture porosity results in an increased in cumulative oil production as shown in Table 5.2.

Fig. 5.5 is as a result of matrix and fracture permeability. Increasing vertical fracture permeability results in earlier breakthrough time at 60 days and also reduces GOR after breakthrough time. Increase in horizontal fracture permeability delays coning breakthrough time till 75 days and also increase GOR after breakthrough time. Increase in horizontal matrix permeability delays coning breakthrough time to 75 days but reduce GOR after breakthrough time compare to the base case. Reducing both horizontal matrix permeability and horizontal fracture permeability plays no significant role in coning tendency. There seems to be no significant effect of vertical matrix permeability. Oil recovery above the base case is only evident in increase in horizontal and vertical fracture permeability due to the increase in the cumulative oil production. **Table 5.3** shows the cumulative production of oil and gas due to effect of matrix and fracture porosity.

Fig. 5.6 shows matrix block size effect. For both an increased and a reduced size of matrix block, no significant effect is observed on breakthrough time and/or GOR after breakthrough time with each simulation run having equal breakthrough time of 65 days. Hence, matrix block have no effect on breakthrough time, GOR and the ultimate oil recovery. **Table 5.4** shows cumulative oil and gas production for effect of matrix block size.

Fig. 5.7 shows the effect of fracture spacing. No significant effect on breakthrough time or GOR after breakthrough time when increasing or reducing fracture spacing. A slight change is only obtained in the cumulative production of oil as shown in **Table 5.5.** The highest spacing of 0.2 ft produces about 636,000 bbls which is higher than the base case of 624,000 bbls while the base case cumulative production of oil is higher than the smallest fracture spacing of 0.001 ft producing 623,000 bbls. **Fig. 5.8** depicts influence of fracture spacing on oil recovery in a naturally fractured reservoir.

Fig. 5.9 shows the effect of vertical to horizontal ratio (Anisotropy ratio) on Field Oil Production Rate (FOPR). Increase in FOPR ratio results to early breakthrough time at 39 days and GOR after breakthrough time while the cumulative oil production is lowered to 426,000 bbls compare to base case of 624,000 bbls, whereas a lower anisotropy ratio delays coning tendency to 282 days and increases cumulative oil production to 855,000 bbls above the base case. **Table 5.6** shows the cumulative oil production oil and gas due to anisotropy ratio effect.

Fig. 5.10 depicts the result of three cases run for perforated interval thickness of the perforated zone. For the layers 1,7 and 1,8 the perforated interval was 8ft. A 4 ft and 14 ft interval thickness was varied and the smaller interval thickness resulted in a longer breakthrough time at 80 days and reduces GOR after breakthrough time compare to the base case. An increased interval thickness results in a long breakthrough time at 75 days and increase GOR after breakthrough time above base case level. From the cumulative oil production of 460,000 bbls and 752,000 bbls for both the 4-ft and 14-ft perforated interval thickness respectively shows that increase in interval thickness increase recovery. **Table 5.7** shows the cumulative oil production due to perforated interval thickness.

Fig. 5.12 shows density difference of oil and/or gas which when increased or reduced delays breakthrough time at 320 days for both simulation runs and also reduces GOR after breakthrough time compare to the base case for same cumulative oil production. **Table 5.8** displays effect of density difference on cumulative oil and gas production.

In **fig. 5.13,** three cases were run to study the effect of mobility ratio. A significant effect on coning tendency is observed when there is a decrease in oil viscosity and an increase in gas viscosity which delays gas breakthrough time to 160 days compare to the 65 days of the base case, reduces GOR after breakthrough time compare to the base case but increases ultimate recovery as evidence in the 675,000 bbls of cumulative oil production compare to that of 624,000 bbls for the base case.

5.1 INFLUENCE OF FRACTURE SYSTEM

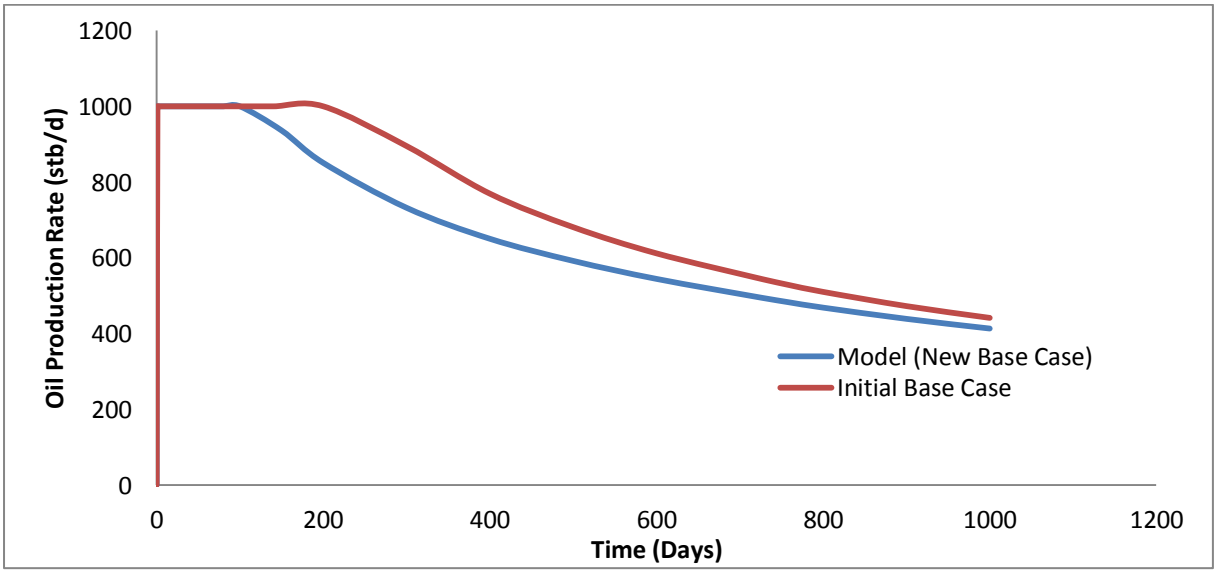

Figure 5.1: Effect of Fracture System in NFR

5.2 OIL FLOW RATE EFFECT

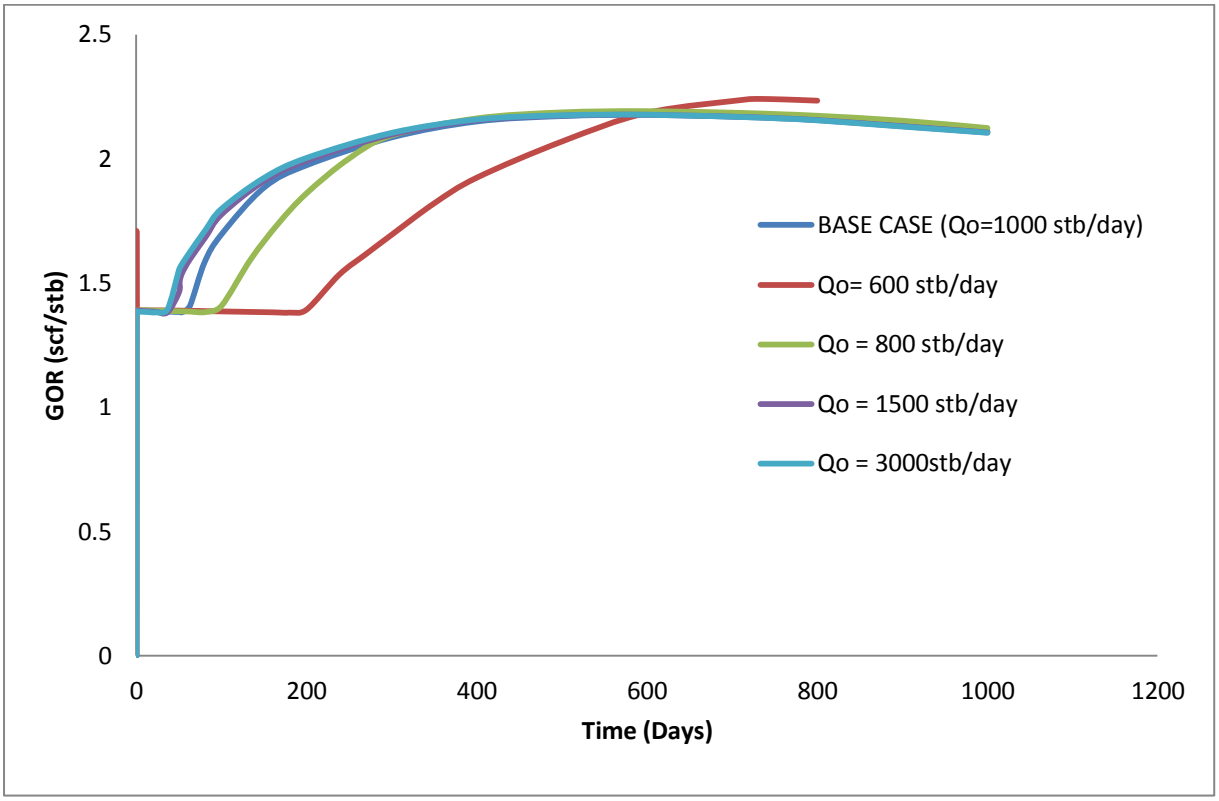

Figure 5.2: Oil Production Rate Effect on GOR in NFR

Fluid Volume Rate	Gas Breakthrough Time	Cumulative Production (bbls × 10^3)	
(stb/day)	(days)	Oil	Gas
600	200	564	1085
800	100	610	1217
1000 (BASE CASE)	65	624	1252
1500	40	629	1264
3000	38	630	1269

Table 5.1: Cumulative oil and gas production until gas breakthrough due to oil flow rate

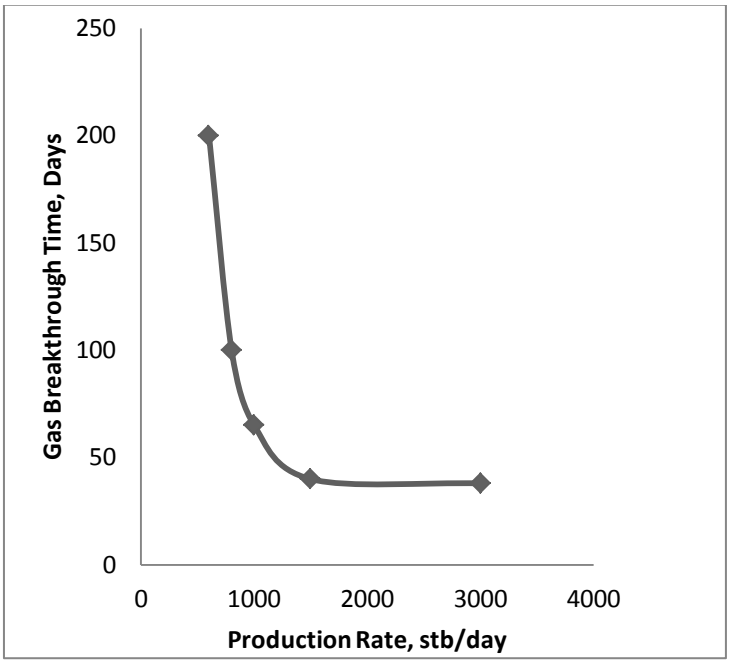

Figure 5.3: Influence of Production Rate on Gas Breakthrough Time in NFR

5.3 POROSITY EFFECT

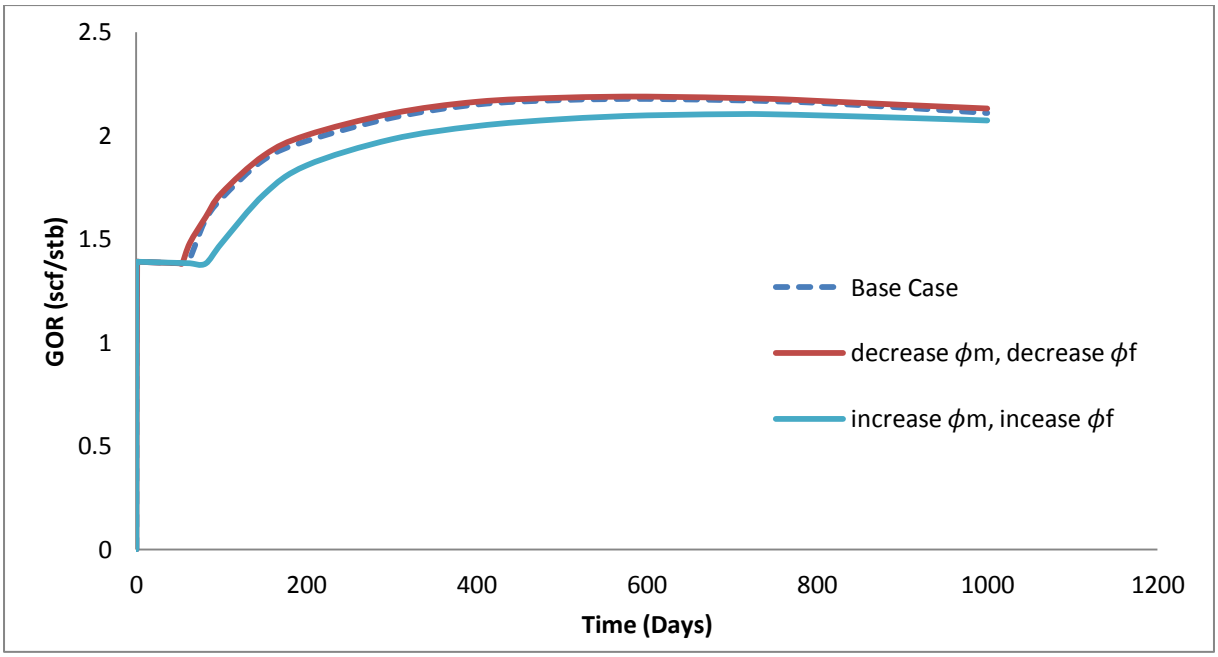

Figure 5.4: Matrix and Fracture Porosity Effect on GOR IN NFR

Porosity	Gas Breakthrough Time	Cumulative Production (bbls × 10^3)	
(%)	(days)	Oil	Gas
$\phi_f = 0.1$ $\phi_m = 0.03$	60	609	1231
$\phi_f = 1.0$ $\phi_m = 0.3$	65	624	1252
$\phi_f = 1.3$ $\phi_m = 0.6$	82	755	1466

Table 5.2: Cumulative oil and gas production until gas breakthrough due to porosity

5.4 MATRIX AND FRACTURE PERMEABILITY EFFECT

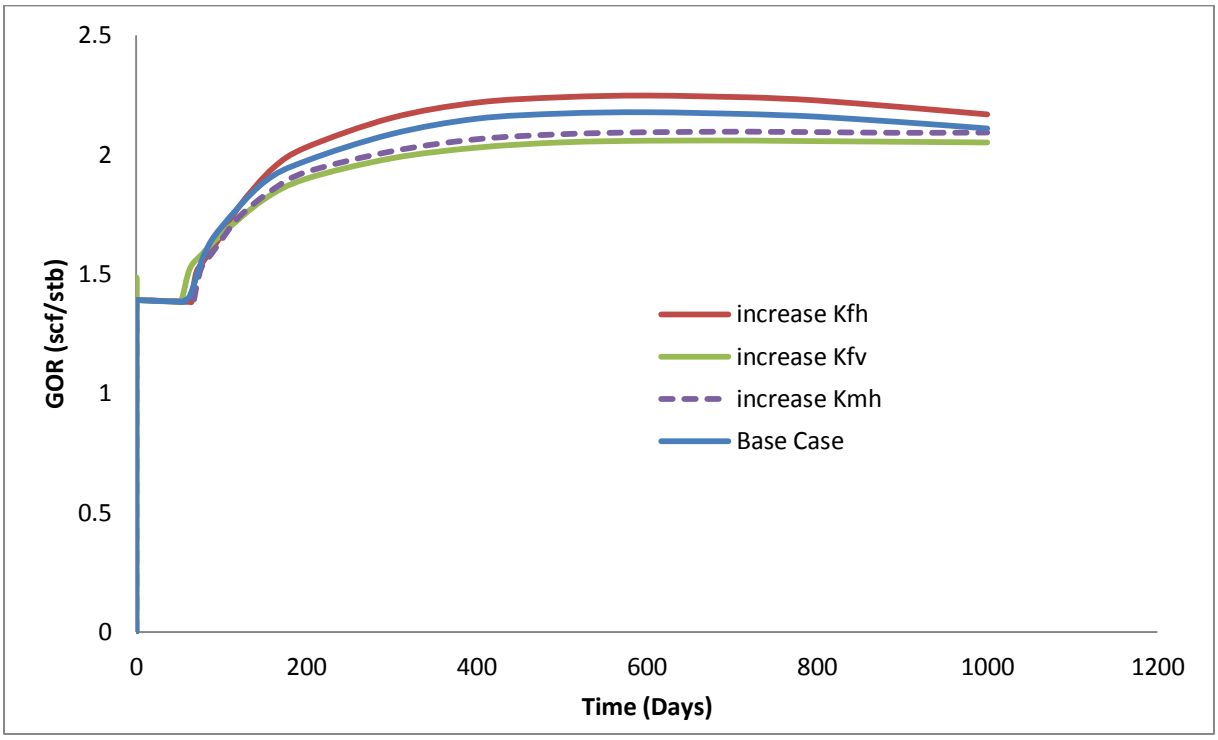

Figure 5.5: Matrix and Fracture Permeability Effect in Horizontal and Vertical direction on GOR IN NFR

Permeability	Gas Breakthrough Time	Cumulative Production (bbls × 10^3)	
(md)	(days)	Oil	Gas
K_{fv} (875)	60	546	1048
K_{mh} (555)	75	608	1179
K_{fh} (954)	75	654	1345
Base Case	65	624	1252

Table 5.3: Cumulative oil and gas production until gas breakthrough, permeability effect

5.5 MATRIX BLOCK-SIZE EFFECT

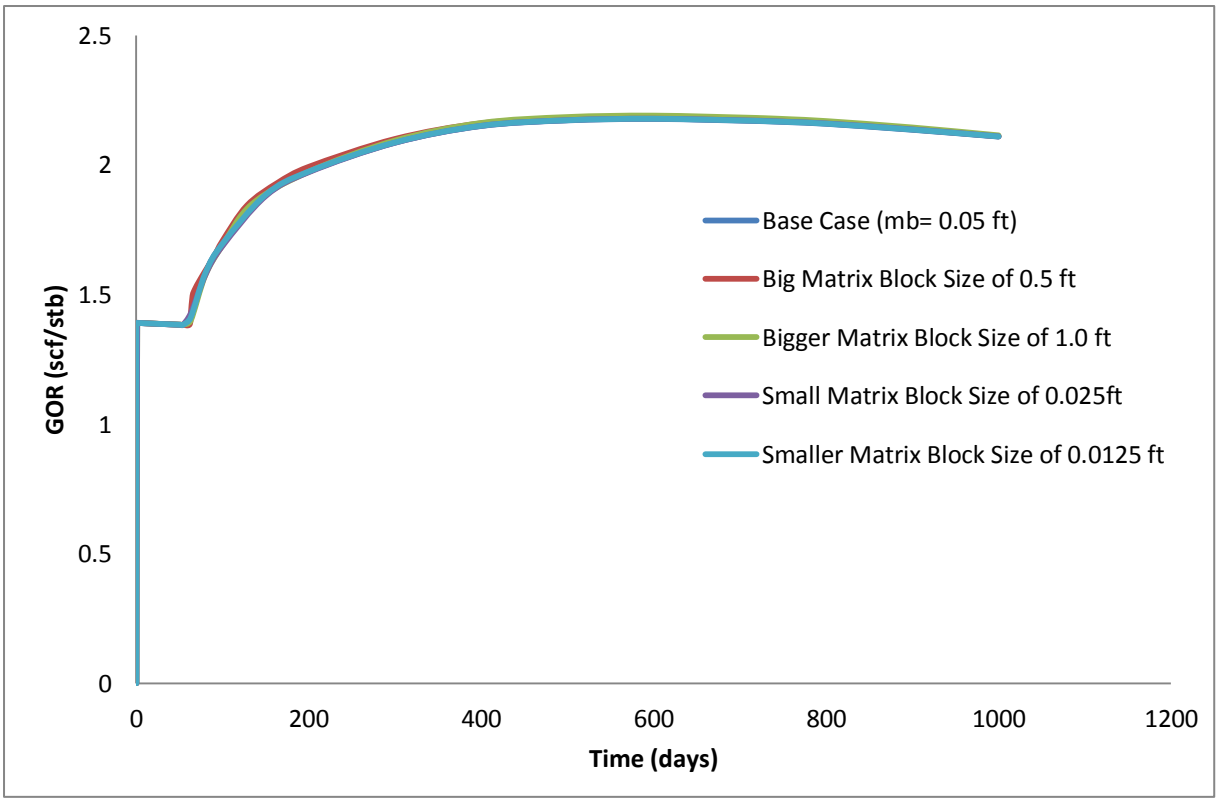

Figure 5.6: Matrix Block Size Effect on GOR IN NFR

Matrix Block Size	Gas Breakthrough Time	Cumulative Production (bbls × 10^3)	
(ft.)	(days)	Oil	Gas
0.0125	65	624	1253
0.0250	65	624	1253
0.05 (BC)	65	624	1252
0.5000	65	624	1254
1.0000	65	624	1259

Table 5.4: Cumulative oil and gas production until gas breakthrough due to matrix block size

5.6 FRACTURE SPACING EFFECT

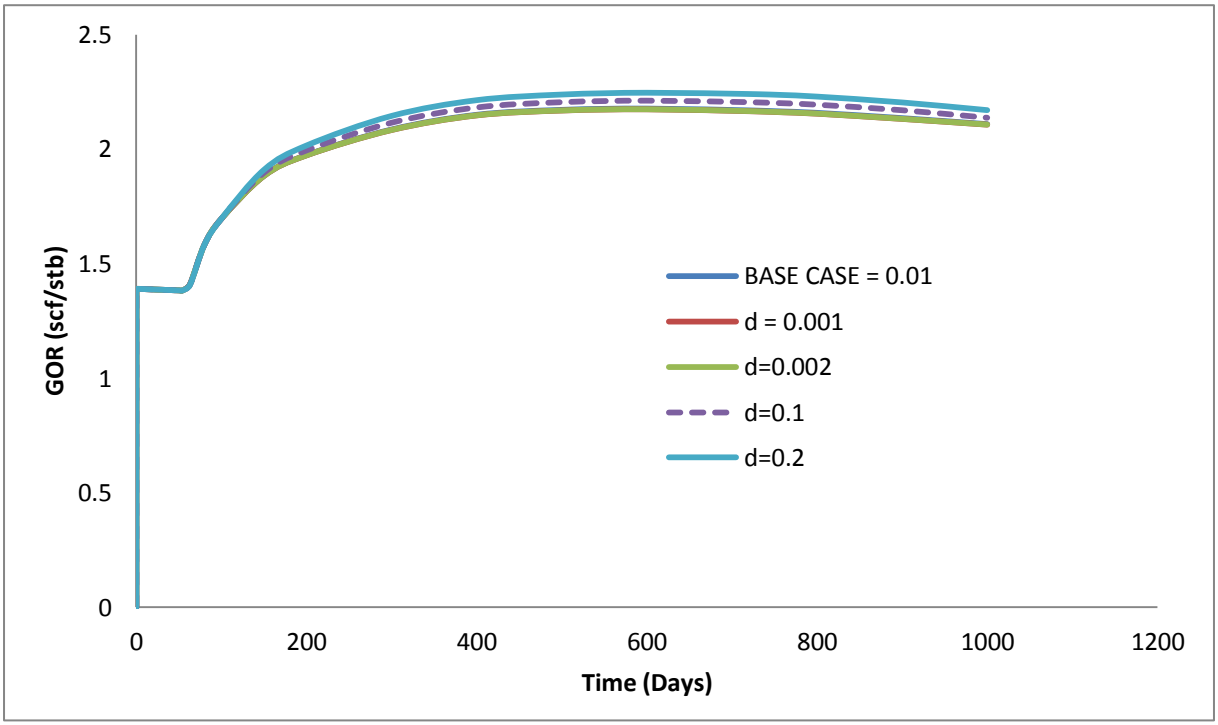

Figure 5.7: Fracture Spacing Effect on GOR in NFR

Fracture Spacing	Gas Breakthrough Time	Cumulative Production (bbls × 10^3)	
(ft.)	(days)	Oil	Gas
0.001	65	623	1249
0.002	65	623	1250
0.01 (BASE CASE)	65	624	1252
0.100	65	630	1280
0.200	65	636	1309

Table 5.5: Cumulative oil and gas production until gas breakthrough due to fracture spacing

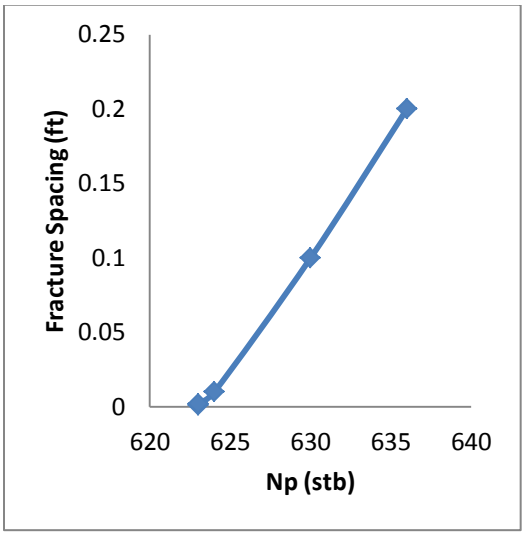

Figure 5.8: Influence of Fracture Spacing on Cumulative Oil Production in NFR

5.7 ANISOTROPY RATIO EFFECT

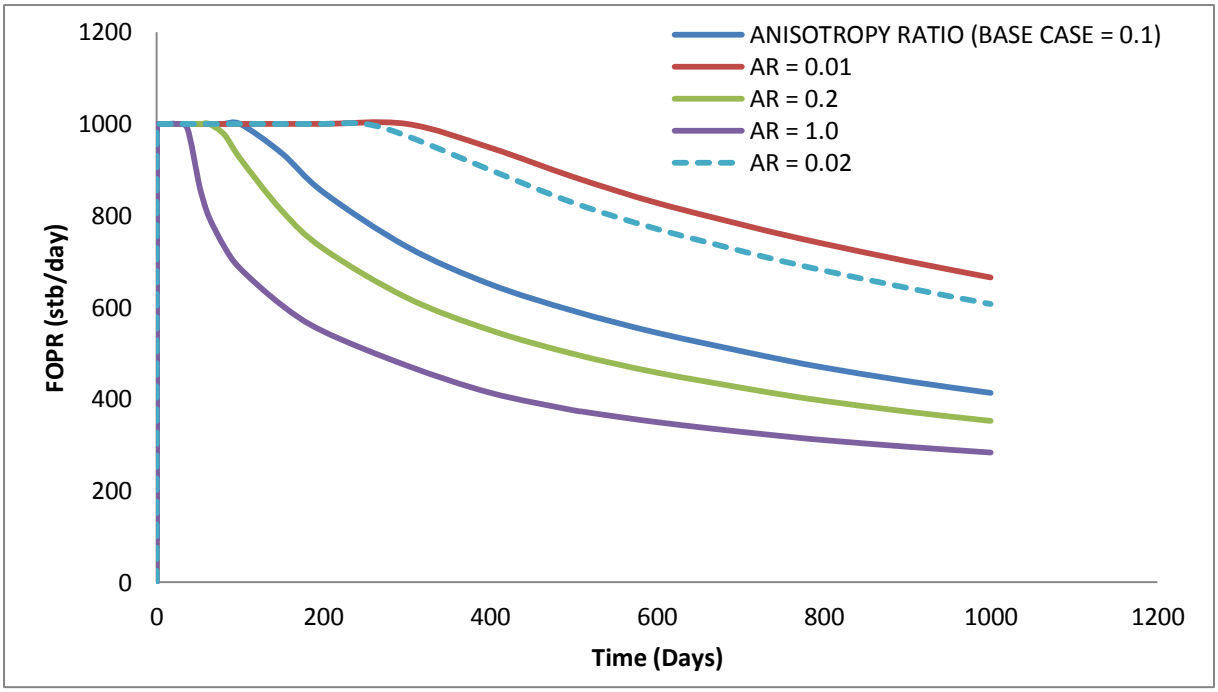

Figure 5.9: Vertical to Horizontal Permeability Ratio Effect on FOPR in NFR

ANISOTROPY RATIO	Gas Breakthrough Time	Cumulative Production (bbls × 10^3)	
	(days)	Oil	Gas
0.01	282	855	1241
0.02	260	814	1273
0.1 (BASE CASE)	100	824	1252
0.200	70	542	1141
1.000	39	426	592

Table 5.6: Cumulative oil and gas production until gas breakthrough, anisotropy ratio effect

5.8 PERFORATED INTERVAL THICKNESS EFFECT

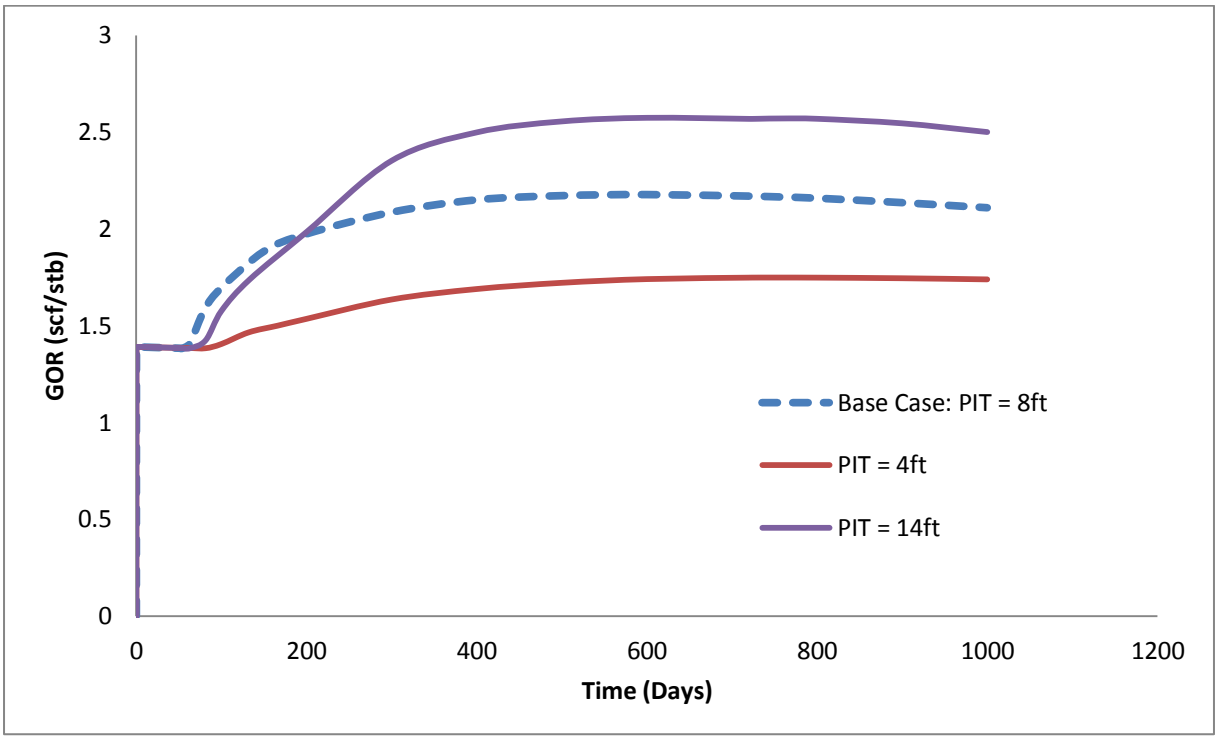

Figure 5.10: Perforated Interval Thickness Effect on GOR IN NFR

Perforated Interval Thickness	Gas Breakthrough Time	Cumulative Production (bbls × 10^3)	
(ft.)	(days)	Oil	Gas
4	80	460	752
8 (BASE CASE)	65	624	1252
14	75	752	1693

Table 5.7: Cumulative oil and gas production until gas breakthrough for PIT

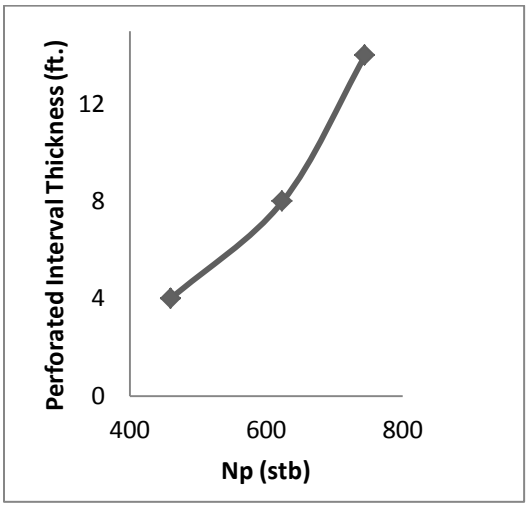

Figure 5.11: Influence of Perforated Interval Thickness on Cumulative Oil Production in NFR

5.9 DENSITY DIFFERENCE EFFECT

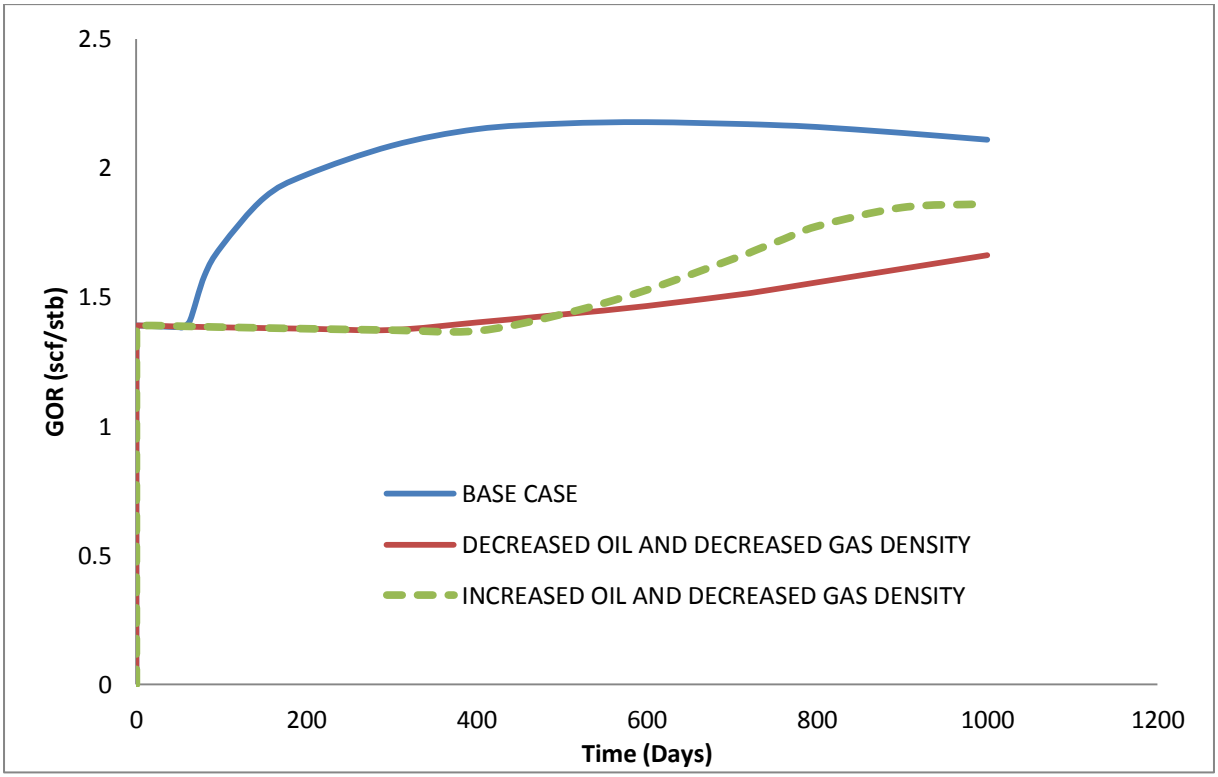

Figure 5.12: Density Difference Effect on GOR IN NFR

DENSITY DIFFERENCE		Gas Breakthrough Time	Cumulative Production (bbls × 10^3)	
lbm/cu ft.	lbm/cu ft.	(days)	Oil	Gas
Oil	Gas			
40	0.00702	320	1000	1476
45	0.070	65	824	1252
55	0.007	320	983	1526

Table 5.8: Cumulative oil and gas production until gas breakthrough due to density difference

5.10 MOBILITY RATIO EFFECT

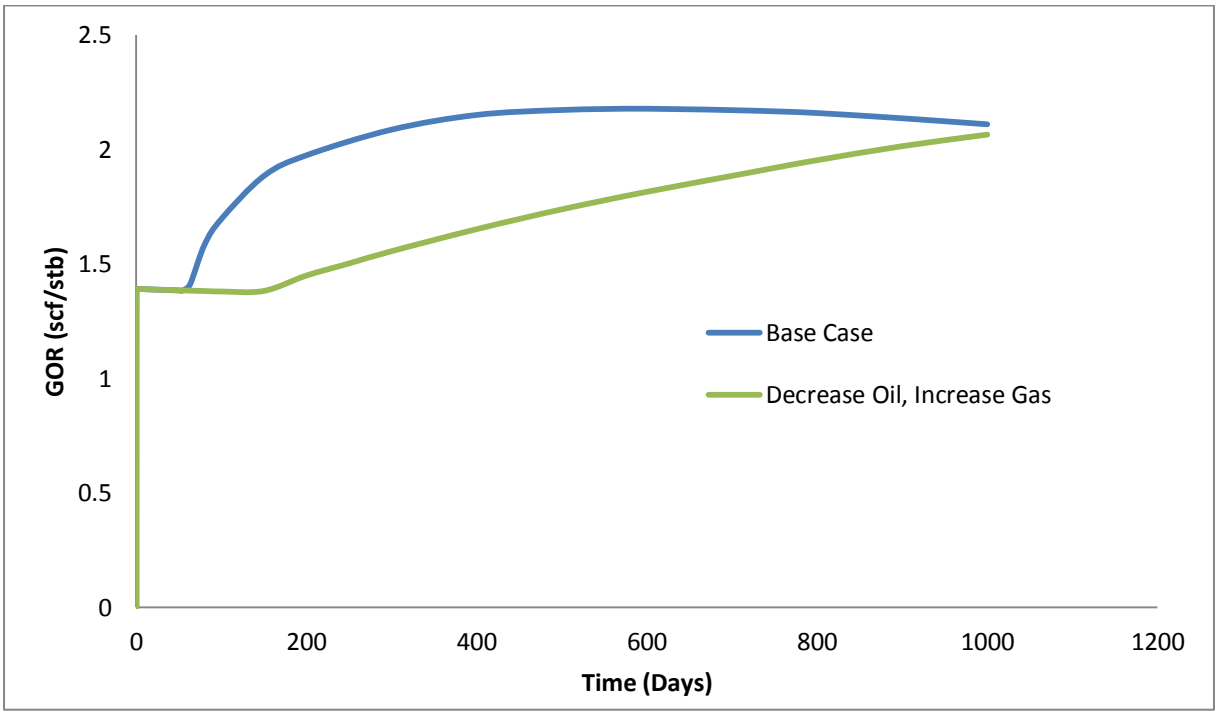

Figure 5.13: Mobility Ratio Effect on GOR IN NFR

Mobility Ratio		Gas Breakthrough Time	Cumulative Production (bbls × 10^3)	
Oil	Gas	(days)	Oil	Gas
0.85 (BC)	0.017 (BC)	65	624	1252
0.950	0.170	160	675	1132

Table 5.9: Cumulative oil and gas production until gas breakthrough due to mobility ratio effect

Figures in appendix A1-A3: As saturation is a variable that is required when assigning values to cells in a reservoir model so is the gas–oil relative permeability a variable required as a function of saturation. As such, gas-oil saturations and a gas-oil relative permeability are plotted in figures in appendix A-1 to A-3 for conditions where cells are very close to the wellbore when coning is happening (block 10 1 7 and block 10 1 8) and where cells are far from wellbore when coning is not happening (block 10 1 1 and block 10 1 2). In figure A-1; the blocks are not affected by coning so oil saturation within the region remains high compare to region where presence of coning reduces oil saturation in fig. A-2. As stated that gas-oil relative permeability is a function of gas saturation, an increase in the gas relative permeability will increase the gas saturation and decreases the oil relative permeability. Matrix and fracture properties greatly influence the gas and oil- saturation. As free gas saturation increases, the oil relative permeability decrease until the oil residual saturation with respect to the gas is reached. Fig. A-3 is gas relative permeability as a function of gas saturation in block 10 1 7 which is close to cell where coning is happening and is greatly affected. The oil relative permeability is influenced in the presence of critical oil saturation while the gas oil relative permeability is taken here in this appendix as negligible in most of the cells because at critical gas saturation, gas relative permeability is zero while oil relative permeability with respect to gas is less than 1.0.

6.0 CONCLUSION AND RECOMMENDATION

6.1 CONCLUSION

A numerical simulation to investigate the effective reservoir parameters of gas coning in a naturally fractured reservoir has being performed. Matrix and fracture properties were modelled to perform the study by modelling a single unit block in a single well radial. A dual-porosity, single-permeability system is used. Sensitivity analysis shows that:

- High flow rate results in early breakthrough but increases ultimate recovery.
- Decrease in matrix and fracture porosity results in early breakthrough time and increases GOR after breakthrough, while an increase in matrix and fracture porosity delays breakthrough time but reduces GOR performance after breakthrough.
- Increase in vertical fracture permeability results to early breakthrough and reduces GOR after breakthrough. Increase in horizontal fracture permeability delays coning breakthrough time and also increase GOR after breakthrough.
- Matrix block have no effect on breakthrough time, GOR and the ultimate oil recovery.
- Fracture spacing have no significant effect on breakthrough time or GOR after breakthrough when increasing or reducing fracture spacing.
- Increase in anisotropy ratio results to early breakthrough time at and GOR after breakthrough, whereas a lower anisotropy ratio delays coning tendency.
- An increased interval thickness results in a long breakthrough time and increase GOR after breakthrough.
- Increased or reduced density difference delays breakthrough time and also reduces GOR after breakthrough.
- A significant effect on coning tendency is observed when there is a decrease in oil viscosity and an increase in gas viscosity which delays gas breakthrough time and reduces GOR after breakthrough but increases ultimate recovery.

6.2 RECOMMENDATION

- Oil viscosity and gas height plays a leading role in coning in naturally fractured reservoir so reservoir management should pay attention to gas arrival time as production rate is increased.

REFERENCES

Ahcene, B. and Djebbar, T.: "Gas Coning in Vertical and Horizontal wells, a Numerical Approach", paper SPE 71026 presented at SPE Rocky Mountain Petroleum Technology Conference, Colorado, May 21-23, 2001.

Behrenbruch, P. and Goda, H.M.: "Two-Phase Relative Permeability Prediction: A comparison of the modified Brooks-Corey Methodology with a New Carman-Kozeny Based Flow Formulation", SPE Asia Pacific Oil and Gas Conference and Exhibition, 11-13 September 2006, Adelaide, Australia.

Birks, J.: "coning theory and its use I predicting allowable producing rates of wells in a fissured limestone reservoir", Iranian Petroleum Institute, no. 12 and 13 (Dec. 1970) 470-480.

Chen Huan–Zhan: "Numerical Simulation of Coning Behaviour of a Single Well in a Naturally Fractured Reservoir", Scientific Research Inst. Of Petroleum Exploration and Developments, December, 1983.

Eclipse Reference Manual, 2008. Schlumberger.

Ershaghi, I. and Al-Afaleg N.I.: "Coning Phenomena in Naturally Fractured Reservoirs", paper SPE 26083 presented at the Western Regional Meeting, Alaska, U.S.A., May 26-28, 1993.

Hasan, A., Foss, B., Sagatun, S.I., Tjostheim, B.P., Svandal, A., and Hatland C.: "Modelling Simulation and Optimal Control of Oil Production under Gas Coning Conditions", 73rd EAGE Conference and Exhibition, 23 – 26 May 2011, Vienna, Austria.

Hasan, A., Sagatun, S. and Foss, B.: "Well Rate Control Design for Gas Coning Problems", Paper presented at the 49th IEEE Conference on Decision and Control, December 15-17, 2010, Atlanta, USA.

Isemin I.A.: "Gravity Drainage Mechanism: Gas-oil displacement in a naturally fractured reservoir" Reservoir Engineering Specialization Project, Department of Petroleum Engineering and Applied Geophysics, Norwegian University of Science and Technology, NTNU-Norway, Autumn, 2011.

Kandil, A.A. and Aggour, M.A.: "Experimental Study of horizontal well performance in fractured reservoirs with bottom-water drive", petroleum science and technology, 2001, pp. 933-947.

Kewen L., Roland N. Horne, Stanford University: "Prediction of Oil Production by Gravity Drainage," SPE 84184, presented at the SPE Annual Technical Conference and Exhibition, Denver Colorado, October 5-8, 2003.

Konieczek, J.: "The Concept of Critical Rate in Gas Coning and its Use in Production Forecasting", paper SPE 20722 presented at the 65th ATCE, New Orleans, LA, Sept. 23-26, 1990.

McDonald, R.C. and Coats, K.H.: "Methods for Numerical Simulation of Water and Gas Coning", paper SPE 2796 presented at Second Symposium on Numerical Simulation of Reservoir Performance, Dallas, Texas, Feb. 5-6, 1970.

Mungan, N.: "A Theoretical and Experimental Coning Study", paper SPE 4982 presented at the SPE-AIME 49th Annual Fall Meeting, Houston, Oct. 6-9, 1974

Papatzacos, P., Herring, T.R., Martinsen, R. and Skjaeveland, S.M.: "Cone Breakthrough Time for Horizontal Wells", SPE Reservoir Engineering, August 1991.

Renard, G., Gadelle, C., Dupuy, J-M., and Alfonso, H.: " Potential of Multilateral Wells in Gas Coning Situations", paper SPE 38760 presented at the 1997 SPE Annual Technical Conference and Exhibition, San Antonio, Texas, Oct. 5-8, 1997.

Ridings, R.L. and Letkeman, J.P.: "A Numerical Coning Model", paper SPE 2812 presented at Second Symposium on Numerical Simulation of Reservoir Performance, Dallas, Texas, Feb. 5-6, 1970.

Shadizadeh, S.R. and Ghorbani, D.: "Investigation of Water/Gas Coning in Naturally Fractured Reservoirs", paper presented at the Petroleum Society's Canadian International Petroleum Conference, Calgary, Alberta, Canada, June 12-14, 2001.

Singhal, A.K.: "Water and Gas Coning Cresting: A Technology Overview", Petroleum Recovery Institute, June 4, 1996.

Spivak, A. and Coat, K.H.: "Numerical Simulation of Coning Using Implicit Production Terms", paper SPE 2595 presented at the SPE 44th Annual Fall Meeting, Denver, Colo., Sept. 28-Oct. 1, 1960.

Stone H.I: "Probability Model for Estimating Three-Phase Relative Permeability", *J. Pet. Tech.* (Feb. 1970), 214-18; *Trans*., AIME, 249.

Tarek Ahmed: "Reservoir Engineering Handbook". Gulf Publishing Company, Houston, Texas, 2000.

Uleberg, K., Torsæter, O. and Kleppe, J.: "A Review of Fluid Flow Mechanisms for Modelling of North Sea Fractured Reservoirs," *Proc.* 1993 RUTH Seminar, Stavanger, Oct. 13-14.

Van Golf-Racht, T.D. and Sonier, F.: "Water-Coning in Fractured Reservoir", paper SPE 28572 presented at the 69th ATCE, Orleans, LA, U.S.A., Sept. 1994.

Wang, Y., Moreno, J., and Harfoushian, J.H.: "Using production logs to calibrate horizontal wells in reservoir simulation", paper SPE 110412 presented at the Asia Pacific Oil and Gas Conference and Exhibition, Jakarta, Indonesia, 2007.

Weinstein, H.G., Chappelear J.E., and Nolen J.S.: "Second Comparative Solution Project: A Three-Phase Coning Study", JPT. Vol. 38, March 1986, pp.345-353.

NOMENCLATURE

A	=	cross - sectional area of core, ft^2
B_o	=	oil formation volume factor, rb/stb
B_g	=	gas formation volume factor, rb/stb
GOR	=	gas-oil ratio
g_a	=	apparent acceleration of gravity in centrifuge
H	=	height of matrix block, ft
h_o	=	oil formation thickness, ft
h_{ap}	=	average oil column height above perforation, ft
h_{bp}	=	average oil column height below perforation, ft
h_p	=	perforated interval thickness, ft
h_{gb}	=	gas breakthrough height, ft
K	=	permeability, md
K_h	=	horizontal permeability, md
K_v	=	vertical permeability, md
K_{ro}	=	oil relative permeability, md
K_{rof}	=	fracture oil relative permeability, md
K_{ro}	=	oil relative permeability, md
L	=	core length, ft
M	=	Gas-oil mobility ratio
m_c	=	gas cap to oil zone ratio
N_p	=	cumulative oil production, stb
$(N_p)_{BT}$	=	cumulative oil production at breakthrough time, stb
n	=	relative permeability exponent
ΔP	=	pressure gradients
P_G	=	gravity pressure
P_{cg}	=	gas capillary pressure
P_{cgo}	=	gas-oil capillary pressure
P_{co}	=	oil capillary pressure
ΔP_g	=	gas pressures
P_{cf}^o	=	threshold capillary pressure for fracture
P_{cf}	=	fracture capillary pressure
$q_{co,v}$	=	vertical well oil production rate, STB/cu ft reservoir-day
$q_{co,h}$	=	horizontal well oil production rate, STB/cu ft reservoir-day
$q_{D,v}$	=	vertical well dimension production rate
$q_{D,h}$	=	horizontal well dimension production rate
q_{vo}	=	oil production, STB/cu ft reservoir-day
q_{vg}	=	gas production, STB/cu ft reservoir-day
q_i	=	initial oil production rate
R	=	recovery
RS	=	solution gas-oil ratio, stb/stb
RS	=	solution gas-oil ratio calculated at the flowing well pressure, stb/stb

r_e	=	drainage radius, ft
r_w	=	wellbore radius, ft
S_g	=	gas saturation, fraction
$\bar{S}_{or}$	=	average residual oil saturation
S_O^*	=	normalized oil saturation
S_o	=	oil saturation, fraction
S_{of}	=	fracture oil saturation
S_{orf}	=	fracture residual oil saturation
S_{wi}	=	initial water saturation
S_{wiorf}	=	initial water oil residual saturation for the fracture
t	=	time, days
t_{BT}	=	breakthrough time, days
Δt	=	time increment, days
Δ_t	=	difference operator with respect to time
z	=	vertical distance measured positively downward, ft
z_D	=	dimensionless height
z_e	=	depth that corresponds with the entry capillary pressure
η	=	recoverable oil recovery
β	=	constant rate of convergence
λ	=	interporosity flow parameter
$\delta\xi$	=	fraction of perforated interval
ξ	=	fraction of oil column height above perforations
ϕ	=	porosity
ϕ_{eff}	=	effective porosity
ϕ_m	=	matrix porosity
Φ	=	flow potential, psia
ρ_o	=	oil density, Ib /cu ft
ρ_g	=	gas density, Ib /cu ft
μ_o	=	oil viscosity phase, cp
μ_g	=	gas viscosity phase, cp
$(T_r)_{i+1/2}$	=	transmissibility for flow in the radial direction between blocks i + 1 and i
$(T_z)_{k+1/2}$	=	Transmissibility for flow in the vertical direction between blocks k + 1 and k

APPENDIX A

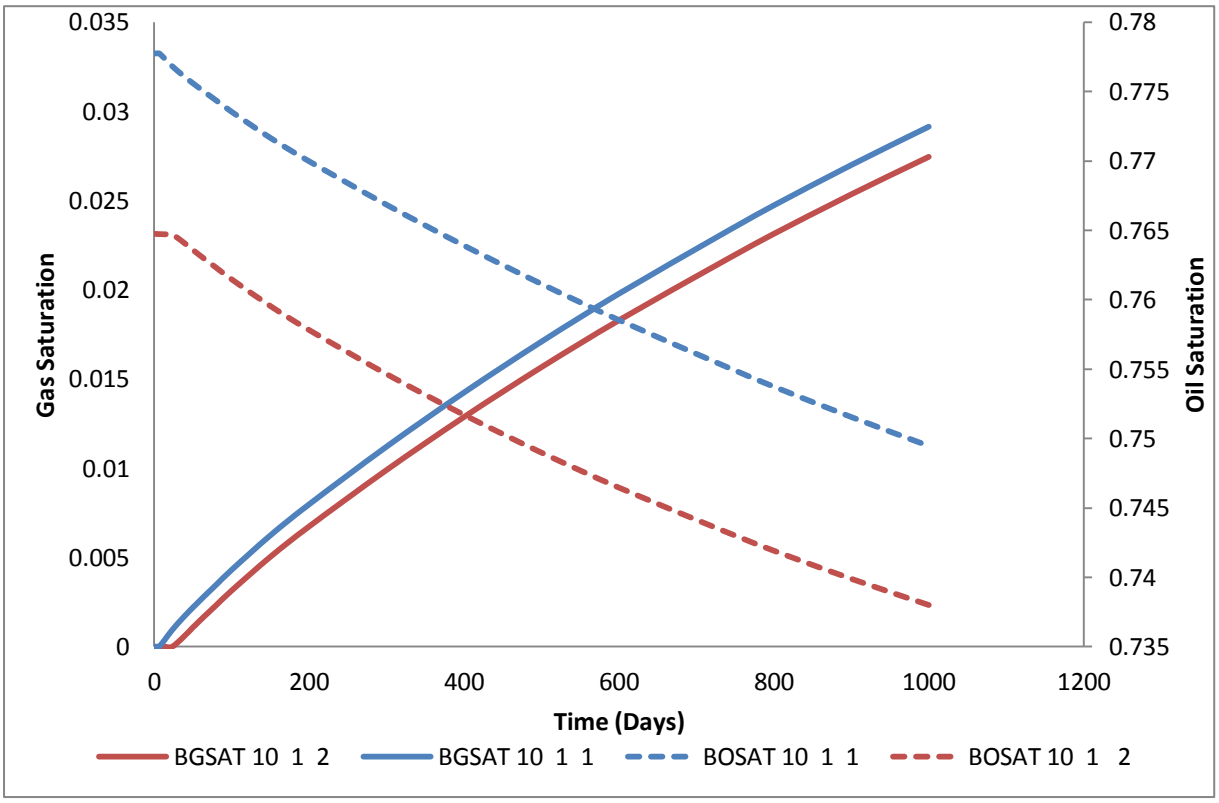

Figure A-1: Gas and Oil saturation as a function of time in Blocks 10 1 1 and 10 1 2

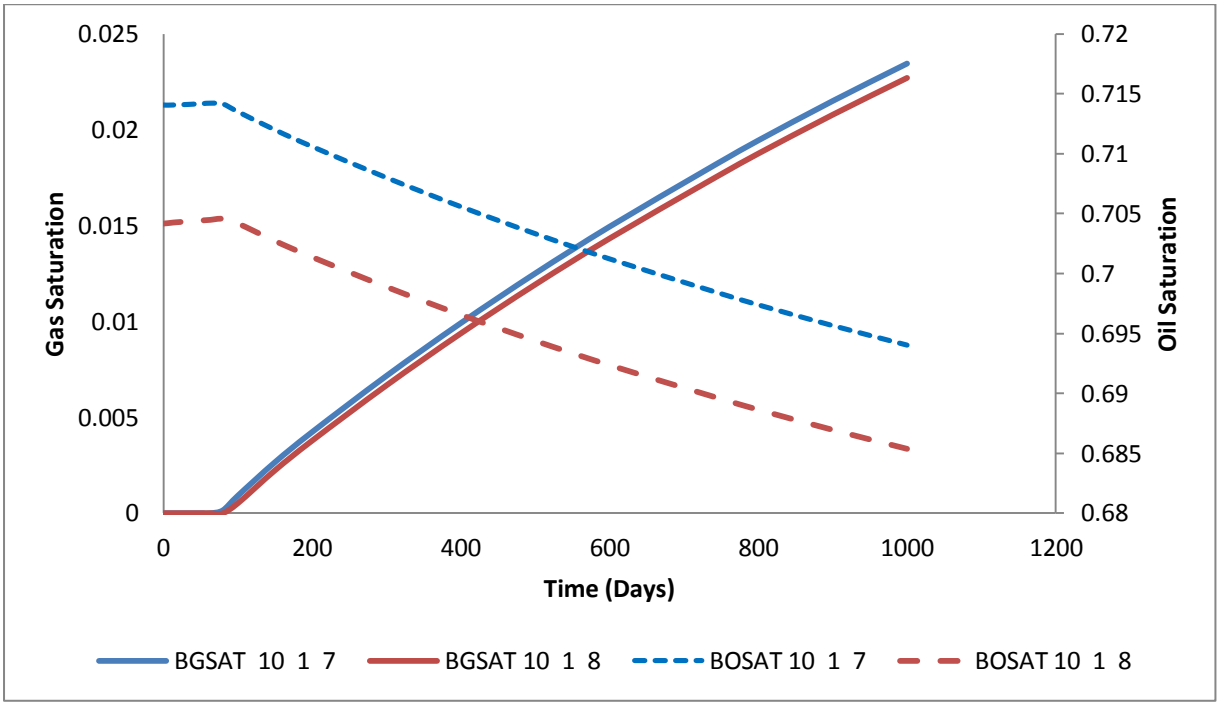

Figure A-2: Gas and Oil saturation as a function of time in Blocks 10 1 7 and 10 1 8

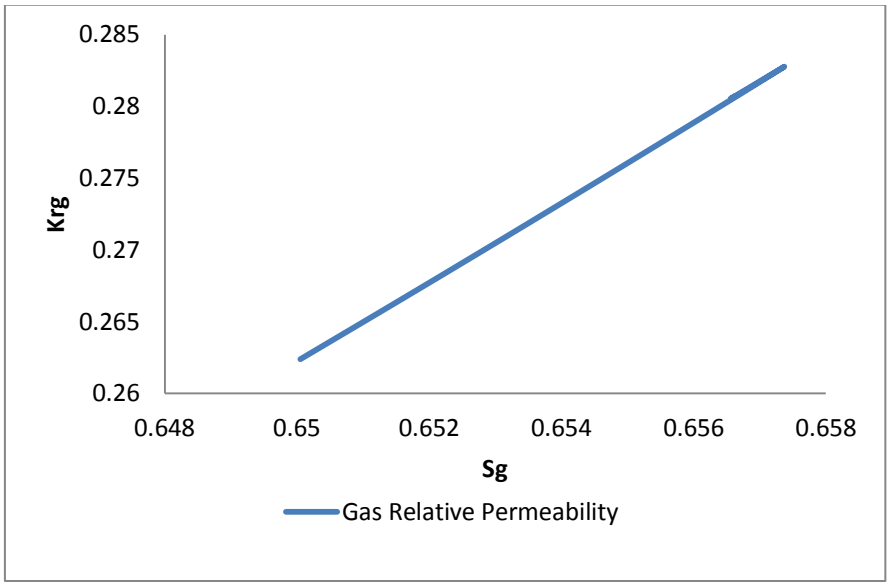

Figure A-3: Gas Relative Permeability as a function of time in Blocks 10 1 7 and 10 1 8

APPENDIX B

```
-- ==================================================================
-- ECLIPSE 100 CHAP TEST DATA (REVISED JULY 1990)
-- NOTE:  THIS DATASET PRODUCES THE OUTPUT FILES TO BE USED FOR
--       TESTING GRAF.  THE PROBLEM IS THE SAME AS THAT IN
--       THE NOIO BENCHMARK EXAMPLE.  THE WELL NAME HAS BEEN
--       CHANGED FROM 'PRODUCER' TO 'P1'. (THE OLD VERSION OF
--       THE CHAP DATASET CAN BE FOUND IN CHAPOLD.DATA)
-- ==================================================================
-- THIS IS THE SECOND SPE COMPARISON PROBLEM , REPORTED BY CHAPPELEAR
-- AND NOLEN AT THE SIXTH SPE SYMPOSIUM ON RESERVOIR SIMULATION , NEW
-- ORLEANS, JANUARY 82 . IT IS  A SINGLE WELL CONING  STUDY , WITH THE
-- WELL CONNECTED TO TWO GRID BLOCKS. DURING THE PRODUCTION SCHEDULE,
-- THE WELL RATE IS SUBJECT TO LARGE CHANGES, AND AT ABOUT 250 DAYS
-- CHANGES FROM FLOW RATE TO BHP CONTROL.
-- ==================================================================
RUNSPEC
TITLE
          Chappelear 3 phase radial coning study

DIMENS
  10   1   15 /

RADIAL

NONNC

OIL

WATER

GAS

DISGAS

FIELD

EQLDIMS
  1  100   10   1   20 /

TABDIMS
  1   1   19   15   15   15 /

REGDIMS
  15   1   0   0 /

WELLDIMS
  1   2   1   1 /

NUPCOL
  4 /
```

```
START


  1 'JAN' 1982  /

NSTACK
  24 /

DEBUG
 2  0  0   0  0  0  1/

--NOSIM

GRID    ================================================================
-------- IN THIS SECTION , THE GEOMETRY OF THE SIMULATION GRID AND THE
-------- ROCK PERMEABILITIES AND POROSITIES ARE DEFINED.
----------------------------------------------------------------------

COLUMNS
 10  60 /
--3456789
      PSEUDO

      SAVE
       /
      COLUMNS
       1  80 /

-- SPECIFY INNER RADIUS OF 1ST GRID BLOCK IN THE RADIAL DIRECTION

INRAD
 0.25 /


--  SPECIFY GRID BLOCK DIMENSIONS IN THE R DIRECTION
DRV
   1.75    2.32    5.01   10.84   23.39
  50.55   109.21   235.92   509.68  1101.08  /


-- SPECIFY CELL THICKNESSES ( DZ ), RADIAL PERMEABILITIES ( PERMR )
-- AND POROSITIES ( PORO ) FOR EACH LAYER OF THE GRID. ALSO CELL TOP
-- DEPTHS ( TOPS ) FOR LAYER 1. DTHETA IS SET TO 360 DEGREES FOR EVERY
-- GRID BLOCK IN THE RESERVOIR.
--    ARRAY    VALUE  ------ BOX ------
EQUALS

    'DTHETA'  360   /  BOX DEFAULTS TO THE WHOLE GRID

    'DZ'     20    1 10  1  1  1  1  /  LAYER 1
    'PERMR'   35    /
```

```
'PORO'   0.087 /
'TOPS'   9000  /

'DZ'    15    1 10  1  1  2  2  / LAYER 2
'PERMR'  47.5  /
'PORO'   0.097 /

'DZ'    26    1 10  1  1  3  3  / LAYER 3
'PERMR'  148   /
'PORO'   0.111 /

'DZ'    15    1 10  1  1  4  4  / LAYER 4
'PERMR'  202   /
'PORO'   0.160 /

'DZ'    16    1 10  1  1  5  5  / LAYER 5
'PERMR'  90    /
'PORO'   0.130 /

'DZ'    14    1 10  1  1  6  6  / LAYER 6
'PERMR'  418.5 /
'PORO'   0.170 /

'DZ'    8     1 10  1  1  7  7  / LAYER 7
'PERMR'  775   /
'PORO'   0.170 /

'DZ'    8     1 10  1  1  8  8  / LAYER 8
'PERMR'  60    /
'PORO'   0.080 /

'DZ'    18    1 10  1  1  9  9  / LAYER 9
'PERMR'  682   /
'PORO'   0.140 /

'DZ'    12    1 10  1  1 10 10  / LAYER 10
'PERMR'  472   /
'PORO'   0.130 /

'DZ'    19    1 10  1  1 11 11  / LAYER 11
'PERMR'  125   /
'PORO'   0.120 /

'DZ'    18    1 10  1  1 12 12  / LAYER 12
'PERMR'  300   /
'PORO'   0.105 /

'DZ'    20    1 10  1  1 13 13  / LAYER 13
'PERMR'  137.5 /
'PORO'   0.120 /

'DZ'    50    1 10  1  1 14 14  / LAYER 14
```

```
    'PERMR'   191   /
    'PORO'    0.116 /

    'DZ'     100    1 10  1  1 15 15  /  LAYER 15
    'PERMR'   350   /
    'PORO'    0.157 /

/   EQUALS IS TERMINATED BY A NULL RECORD

--  COPY RADIAL PERMEABILITIES ( PERMR ) INTO VERTICAL PERMEABILITIES
--  ( PERMZ ) FOR THE WHOLE GRID, AND THEN MULTIPLY PERMZ BY 0.1.
-------- SOURCE     DESTINATION
COPY
      'PERMR'     'PERMZ'     /
/
-------- ARRAY     FACTOR
MULTIPLY
     'PERMZ'     0.1    /
/

-- OUTPUT OF CELL DIMENSIONS, PERMEABILITIES, POROSITY AND TOPS
-- DATA IS REQUESTED, AND OF THE CALCULATED PORE VOLUMES, CELL
-- CENTRE DEPTHS AND X AND Z DIRECTION TRANSMISSIBILITIES
RPTGRID
 1  1  1  1  0  1  0  0  0  1  0  1  1  1  1  0  1 /

PROPS   ================================================================
-------- THE PROPS SECTION DEFINES THE REL. PERMEABILITIES, CAPILLARY
-------- PRESSURES, AND THE PVT PROPERTIES OF THE RESERVOIR FLUIDS
----------------------------------------------------------------------
-- WATER RELATIVE PERMEABILITY AND CAPILLARY PRESSURE ARE TABULATED AS
-- A FUNCTION OF WATER SATURATION.
--
--  SWAT   KRW   PCOW
SWFN

   0.22  0      7
   0.3   0.07   4
   0.4   0.15   3
   0.5   0.24   2.5
   0.6   0.33   2
   0.8   0.65   1
   0.9   0.83   0.5
   1     1      0     /

-- SIMILARLY FOR GAS
--
--  SGAS   KRG   PCOG
SGFN      1 TABLES   19 NODES IN EACH         FIELD   16:31 18 JAN 85
   .0000  .0000  .0000
   .0400  .0000  .2000
   .1000  .0220  .5000
```

```
   .2000  .1000 1.0000
   .3000  .2400 1.5000
   .4000  .3400 2.0000
   .5000  .4200 2.5000
   .6000  .5000 3.0000
   .7000  .8125 3.5000
   .7800 1.0000 3.9000
/

-- OIL RELATIVE PERMEABILITY IS TABULATED AGAINST OIL SATURATION
-- FOR OIL-WATER AND OIL-GAS-CONNATE WATER CASES
--
-- SOIL    KROW    KROG
SOF3
   0       0                0
   0.2     0                0
   0.38    0.00432          0
   0.4     0.0048           0.004
   0.48    0.05288           0.02
   0.5     0.0649           0.036
   0.58    0.11298          0.1
   0.6     0.125            0.146
   0.68    0.345            0.33
   0.7     0.4              0.42
   0.74    0.7              0.6
   0.78     1               1       /


-- PVT PROPERTIES OF WATER
--
--   REF. PRES. REF. FVF  COMPRESSIBILITY  REF VISCOSITY  VISCOSIBILITY
PVTW
      3600     1.00341       3.0D-6        0.96          0  /


-- ROCK COMPRESSIBILITY
--
--   REF. PRES   COMPRESSIBILITY
ROCK
      3600        4.0D-6   /

-- SURFACE DENSITIES OF RESERVOIR FLUIDS
--
--      OIL   WATER   GAS
DENSITY
       45   63.02   0.0702  /

-- PVT PROPERTIES OF DRY GAS (NO VAPOURISED OIL)
-- WE WOULD USE PVTG TO SPECIFY THE PROPERTIES OF WET GAS
--
--   PGAS   BGAS   VISGAS
PVDG
```

```
   400   5.9   0.013
   800   2.95  0.0135
  1200   1.96  0.014
  1600   1.47  0.0145
  2000   1.18  0.015
  2400   0.98  0.0155
  2800   0.84  0.016
  3200   0.74  0.0165
  3600   0.65  0.017
  4000   0.59  0.0175
  4400   0.54  0.018
  4800   0.49  0.0185
  5200   0.45  0.019
  5600   0.42  0.0195 /

-- PVT PROPERTIES OF LIVE OIL (WITH DISSOLVED GAS)
-- WE WOULD USE PVDO TO SPECIFY THE PROPERTIES OF DEAD OIL
--
-- FOR EACH VALUE OF RS THE SATURATION PRESSURE, FVF AND VISCOSITY
-- ARE SPECIFIED. FOR RS=1.81  THE FVF AND VISCOSITY OF
-- UNDERSATURATED OIL ARE DEFINED AS A FUNCTION OF PRESSURE. DATA
-- FOR UNDERSATURATED OIL MAY BE SUPPLIED FOR ANY RS, BUT MUST BE
-- SUPPLIED FOR THE HIGHEST RS (1.81).
--
--  RS    POIL   FVFO   VISO
PVTO
  0.165    400  1.012   1.17  /
  0.335    800  1.0255  1.14  /
  0.500   1200  1.038   1.11  /
  0.665   1600  1.051   1.08  /
  0.828   2000  1.063   1.06  /
  0.985   2400  1.075   1.03  /
  1.130   2800  1.087   1.00  /
  1.270   3200  1.0985  0.98  /
  1.390   3600  1.11    0.95  /
  1.500   4000  1.12    0.94  /
  1.600   4400  1.13    0.92  /
  1.676   4800  1.14    0.91  /
  1.750   5200  1.148   0.9   /
  1.810   5600  1.155   0.89
          6000  1.1504  0.89
          6400  1.1458  0.89
          6800  1.1412  0.89
          7200  1.1367  0.89  /
/

-- SWITCH ON OUTPUT OF ALL PROPS DATA
RPTPROPS
 8*1  /

REGIONS  ====================================================================
-------- THE REGIONS SECTION DEFINES HOW THE RESERVOIR IS SPLIT INTO
```

```
-------- REGIONS BY SATURATION FUNCTION, PVT FUNCTION, FLUID IN PLACE
-------- REGION ETC.
---------------------------------------------------------------------
FIPNUM
 10*1  10*2  10*3  10*4  10*5  10*6  10*7  10*8  10*9  10*10
 10*11 10*12 10*13 10*14 10*15  /

-- SWITCH ON OUTPUT OF FIPNUM
RPTREGS
 0 0 0 1 /

SOLUTION ====================================================================
-------- THE SOLUTION SECTION DEFINES THE INITIAL STATE OF THE SOLUTION

-------- VARIABLES (PHASE PRESSURES, SATURATIONS AND GAS-OIL RATIOS)
---------------------------------------------------------------------
-- DATA FOR INITIALISING FLUIDS TO POTENTIAL EQUILIBRIUM
--
--   DATUM  DATUM   OWC    OWC    GOC    GOC    RSVD   RVVD   SOLN
--   DEPTH  PRESS  DEPTH   PCOW  DEPTH   PCOG  TABLE  TABLE   METH
EQUIL
    9035   3600   9209   0    9035   0      0     0  /

-- SWITCH ON OUTPUT OF INITIAL SOLUTION
RPTSOL                              FIELD   16:05 12 DEC 88
  1  0  1  1  1  0  2  1  1  0  0  0  0  0  0  0  0
  0  0  0  0  0  0  0  0  0  0  0  0  0  0  0  0  0
  0  0  0  0  0  0  0  0  0  0  0  0  0  0  0  0  /

SUMMARY =====================================================================
-------- THIS SECTION SPECIFIES DATA TO BE WRITTEN TO THE SUMMARY FILES
-------- AND WHICH MAY LATER BE USED WITH THE ECLIPSE GRAPHICS PACKAGE
---------------------------------------------------------------------

-- FIELD Rates for Oil, Water, Liquid & 3 Phase Voidage
FOPR
FWPR
FLPR
FVPR

-- BOTTOM HOLE PRESSURE FOR WELL
WBHP
'P1'
/
-- FIELD Water Cut, GOR and Pressure
FWCT
FGOR
FPR

-- SWITCH ON REPORT OF WHAT IS TO GO ON THE SUMMARY FILES
RPTSMRY
 1  /
```

```
SCHEDULE ================================================================
-------- THE SCHEDULE SECTION DEFINES THE OPERATIONS TO BE SIMULATED
--------------------------------------------------------------------------
-- CONTROLS ON OUTPUT AT EACH REPORT TIME
RPTSCHED                          FIELD   16:07 12 DEC 88
  1  0  1  1  0    0  2  2  2  0    0  2  0  0  0
  0  0  0  0  0    0  0  0  0  0    0  0  0  0  0
  0  0  0  0  0    0  0  0  1  0    0  0  0  0  0 /

-- FREE GAS IS NOT ALLOWED TO DISSOLVE IN UNDERSATURATED OIL
DRSDT
 0.0 /

-- WELL SPECIFICATION DATA

--
--    WELL   GROUP LOCATION  BHP   PI
--    NAME   NAME    I  J   DEPTH DEFN
WELSPECS                          FIELD   16:32 18 JAN 85
'P1','G      ',  1,  1,9110.00,'OIL' /
/

-- COMPLETION SPECIFICATION DATA
--
--    WELL     -LOCATION- OPEN/ SAT CONN
--    NAME     I  J K1 K2 SHUT  TAB FACT
COMPDAT
   'P1'  1  1  7  7 'OPEN' 0  27.228  /
   'P1'  1  1  8  8 'OPEN' 0  2.1079  /
 /

-- PRODUCTION WELL CONTROLS - OIL RATE IS SET TO 1000 BPD
--
--     WELL    OPEN/  CNTL   OIL  WATER   GAS  LIQU   RES   BHP
--     NAME    SHUT   MODE  RATE   RATE  RATE  RATE  RATE
WCONPROD
   'P1'  'OPEN' 'ORAT' 1000   4*                3000  /
 /

-- SPECIFY UPPER LIMIT OF 1 DAY FOR NEXT TIME STEP
TUNING
 1  /
/
 12 1 50 /

-- SPECIFY REPORT AT 10 DAYS
TSTEP
 10.00000
/

-- CUT OIL RATE TO 100 BPD
```

```
WELTARG
'P1', 'ORAT'  100.000000 /
/

-- SPECIFY UPPER LIMIT OF 1 DAY FOR NEXT TIME STEP
TUNING
  1  /
/
 12 1 50 /

-- ADVANCE SIMULATION TO 50 DAYS
TSTEP
 40.00000
/

-- PUT OIL RATE BACK TO 1000 BPD

WELTARG
'P1', 'ORAT'  1000.00000 /
/

-- SPECIFY UPPER LIMIT OF 1 DAY FOR NEXT TIME STEP
TUNING
  1  /
/
 12 1 50 /


-- AND ADVANCE TO 720 DAYS - WELL SWITCHES TO BHP CONTROL AT 250 DAYS
TSTEP
 50.00000  100.0000  100.0000  100.0000  100.0000  100.0000  120.0000
/

-- CUT OIL RATE TO 100 BPD
WELTARG
'P1', 'ORAT'  100.000000 /
/

-- SPECIFY UPPER LIMIT OF 1 DAY FOR NEXT TIME STEP
TUNING
  1  /
/
 12 1 50 /

-- ADVANCE TO 800 DAYS
TSTEP
 80.00000
/

-- RESET OUTPUT CONTROLS TO GET FULL OUTPUT FOR LAST REPORT
RPTSCHED
   1   1   1   1   1   1   2   2   2   1   2   2   1   1   2   /
```

```
-- ADVANCE TO END OF SIMULATION (900 DAYS)
TSTEP
 100.0000
/

END     ============================================================
```

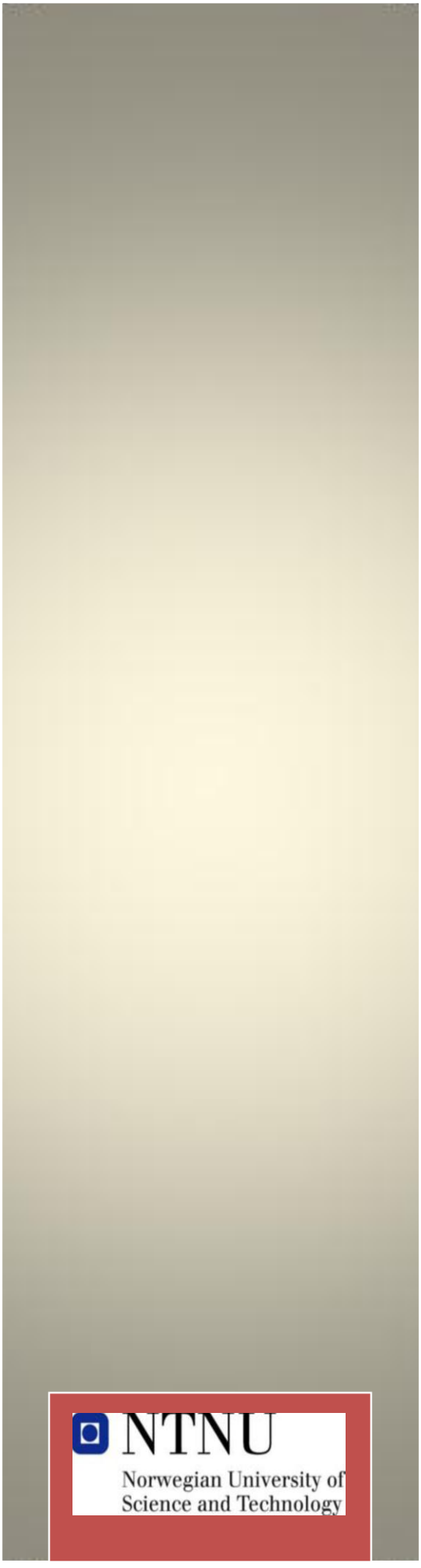
NTNU
Norwegian University of
Science and Technology